Applications of Resistive Wall Model in M3D-C1

by

Nate Ferraro

General Atomics

(now at Princeton Plasma Physics Laboratory)

Presented at the

CEMM Meeting
Savannah, GA

November 15, 2015

Disruption Physics Depends Crucially on Electromagnetic Interaction Between Plasma and External Conductors

- **Interaction between plasma fields and non-axisymmetric external currents causes disruptive instabilities**
  - Error field penetration / Mode Locking
    - Torque brakes plasma → disruptive instability
  - Resistive Wall Modes (RWMs)
    - Finite wall resistivity allows kink instability that would be stabilized by perfectly conducting wall
- **Dynamics of consequent disruption is strongly affected by interaction between plasma and wall**
  - Large displacement of plasma current requires magnetic flux to penetrate wall
  - Strong currents can be driven in external conductors (e.g. vessel) leading to potentially dangerous forces

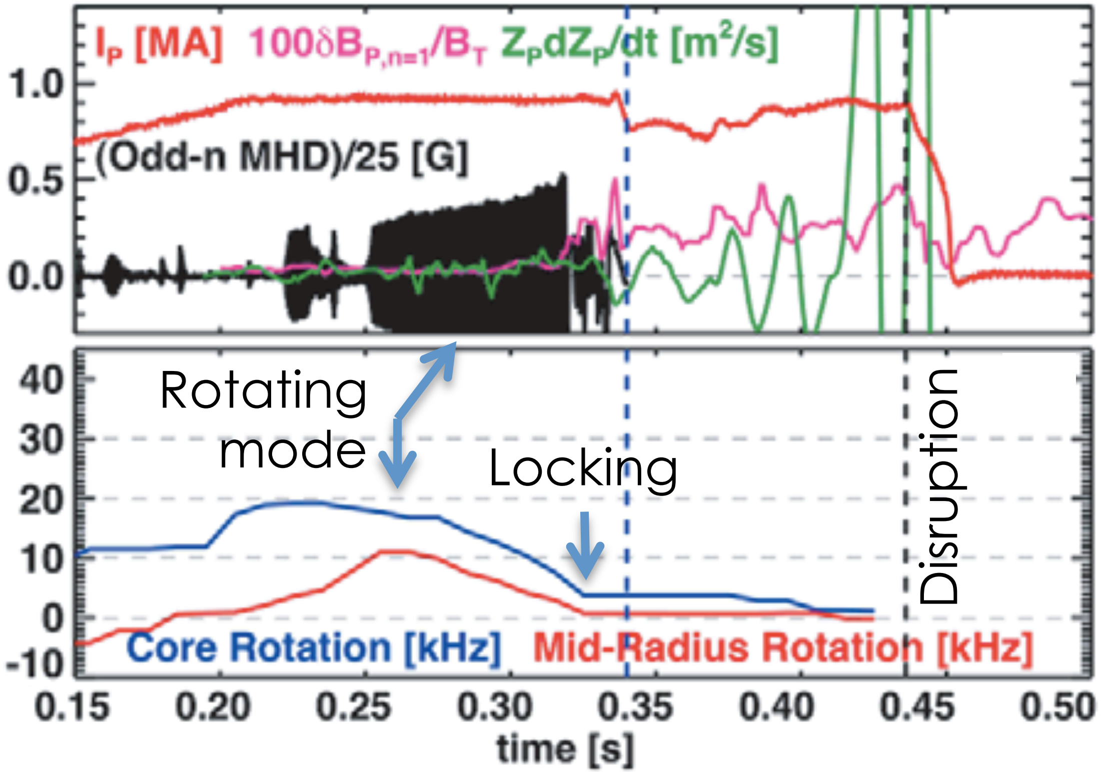

Gerhardt, *et al.*
Nucl. Fusion **53,** 063021

Outline

- **Resistive Wall Model in M3D-C1**
- **Verification Using Analytic Linear Resistive Wall Mode (RWM)**
- **Free-Boundary Perturbed Equilibria**
- **Vertical Displacement Event (VDE) Disruption**

New Resistive Wall Capability In M3D-C1 Includes Resistive Wall In Simulation Domain

- **3 regions inside domain:**
  - XMHD (Extended MHD, includes open field-line region)
  - RW ($\mathbf{E} = \eta_W \mathbf{J}$)
  - Vacuum ($\mathbf{J} = 0$)
- **Boundary conditions:**
  - $\mathbf{v}$, p, n set at inner wall
  - $\mathbf{B}$ set at outer (superconducting) wall
- ***<u>There are no boundary conditions on $\mathbf{B}$ or $\mathbf{J}$ at the resistive wall</u>***
  - Current can flow into and through the resistive wall
- **All regions advanced simultaneously with implicit time step**

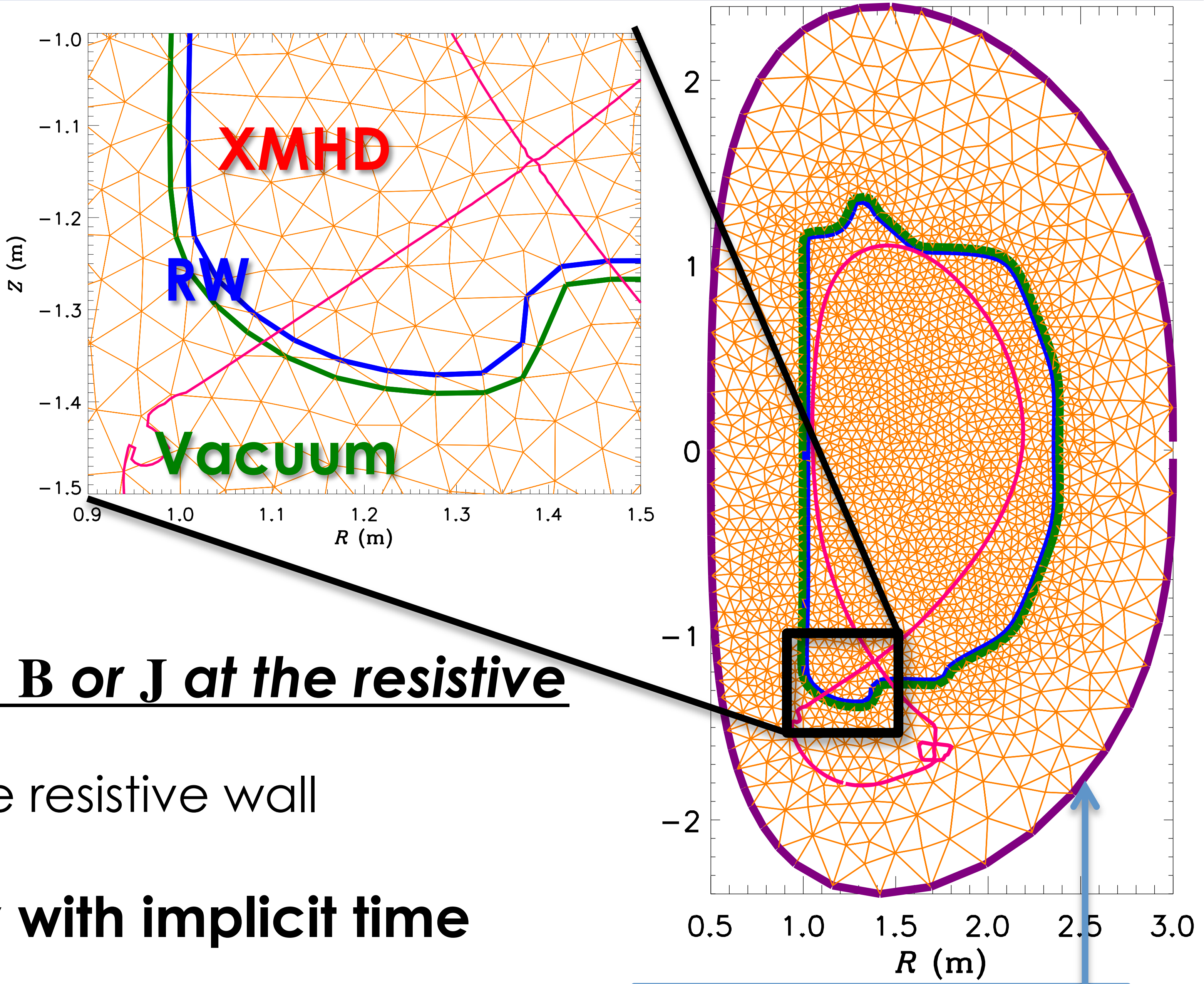

Superconducting Wall

Including Wall in Finite Element Mesh Has Advantages over Boundary Condition Methods

- **Implementing resistive wall as boundary condition introduces non-local coupling**
  - Tangential **B** at *any* point on the wall is a function of normal **B** at *every* point on the wall
  - Introduces communication among non-adjacent domains when parallelized

- **Including wall in the domain has significant advantages:**
  - Avoids non-local coupling (should improve scalability of implicit time-step)
  - Facilitates implementation of plasma/material interaction models

- **Including wall in the domain has some potential disadvantages:**
  - Less modularity (e.g. hard to represent wall with CAD model)
  - Bigger domain (obviated by mesh packing; non-stiff vacuum equations)

Full, Compressible, Two-Fluid Model is Implemented in XMHD Region

$$\frac{\partial n}{\partial t} + \nabla \cdot \left(n_i \mathbf{v} \right) = 0$$

$$n_i m_i \left(\frac{\partial \mathbf{v}}{\partial t} + \mathbf{v} \cdot \nabla \mathbf{v} \right) = \mathbf{J} \times \mathbf{B} - \nabla p - \nabla \cdot \Pi_i$$

$$\frac{\partial p}{\partial t} + \mathbf{v} \cdot \nabla p + \Gamma p \nabla \cdot \mathbf{v} = -\frac{1}{n_e e} \mathbf{J} \cdot \left(\Gamma p_e \frac{\nabla n_e}{n_e} - \nabla p_e \right) - \left(\Gamma - 1 \right) \nabla \cdot \mathbf{q}$$

$$\frac{\partial \mathbf{B}}{\partial t} = -\nabla \times \mathbf{E}$$

$$\mathbf{E} = -\mathbf{v} \times \mathbf{B} + \eta \mathbf{J} + \frac{1}{n_e e} \left(\mathbf{J} \times \mathbf{B} - \nabla p_e \right)$$

$$\Pi_i = -\mu \left[\nabla \mathbf{v} + \left(\nabla \mathbf{v} \right)^T \right] + \Pi_i^{gv} + \Pi_i^{\parallel}$$

$$\mathbf{q} = -\kappa \nabla T_i - \kappa_{\parallel} \mathbf{bb} \cdot \nabla T_e$$

$$\mathbf{J} = \nabla \times \mathbf{B}$$

$$\Gamma = 5/3$$

$$n_e = Z_i n_i$$

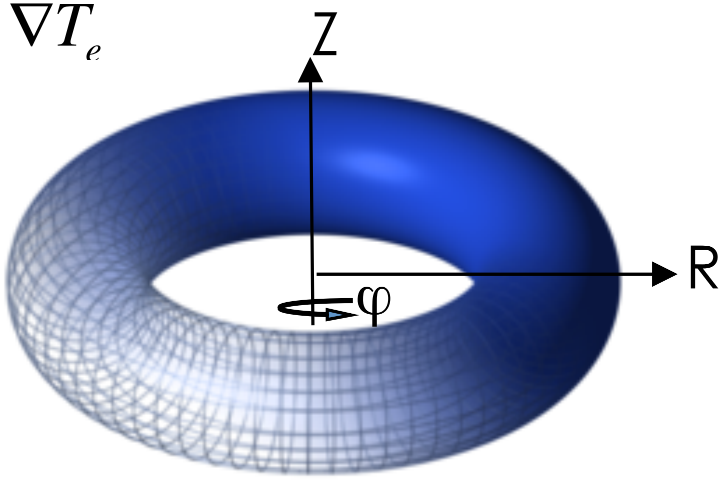

- **(R, φ, Z) coordinates → no coordinate singularities in plasma**
- **Three modes of operation:**
  - Linear, time-dependent (**linear stability**)
  - Linear, time-independent (**perturbed equilibrium**)
  - Nonlinear, time-dependent (**nonlinear dynamics**)

Outline

- Resistive Wall Model in M3D-C1
- **Verification Using Analytic Linear Resistive Wall Mode (RWM)**
- Free-Boundary Perturbed Equilibria
- Vertical Displacement Event (VDE) Disruption

Resistive Model Verified Against Analytic Resistive Wall Mode Result

- **Circular cross-section, cylindrical plasma with constant q, current density (J_z) and mass density (ρ_0) (Shafranov equilibrium)**

- **Analytic thin-wall solution provided by Liu *et al.* *Phys. Plasmas* 15, 072516 (2008)**

Wall time: $\tau_W = \mu_0 bd/(2\eta_W)$
Alfven time: $\tau_A = (\mu_0 \varrho_0)^{1/2} R_0/B_0$

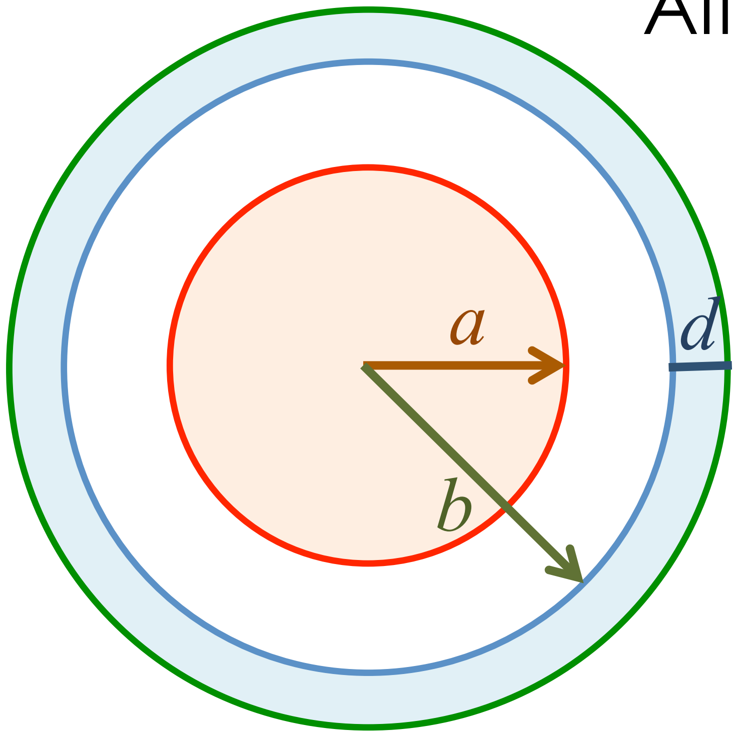

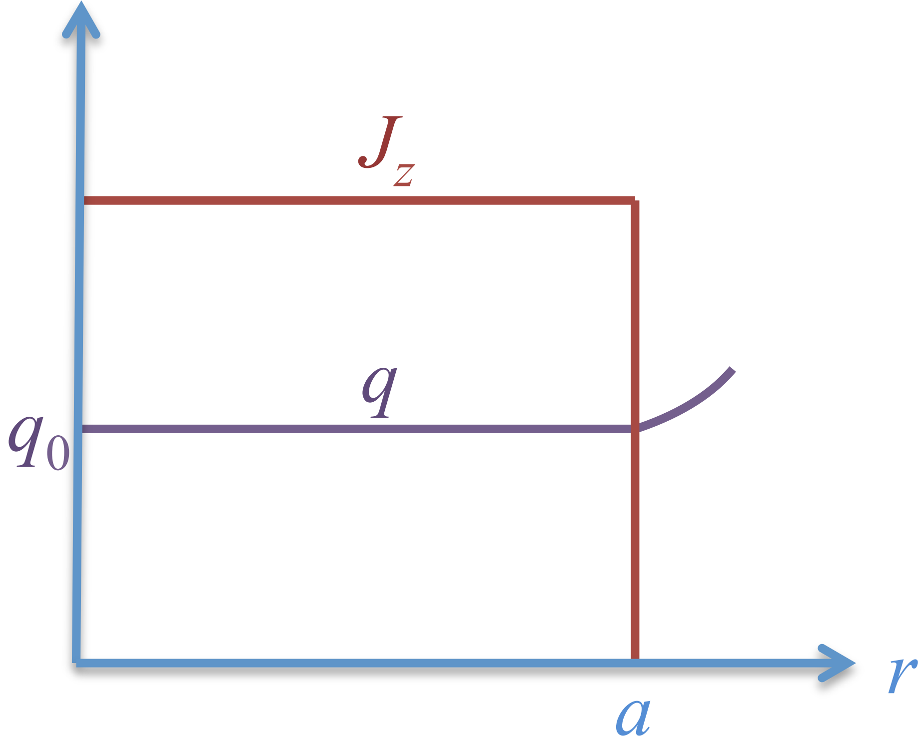

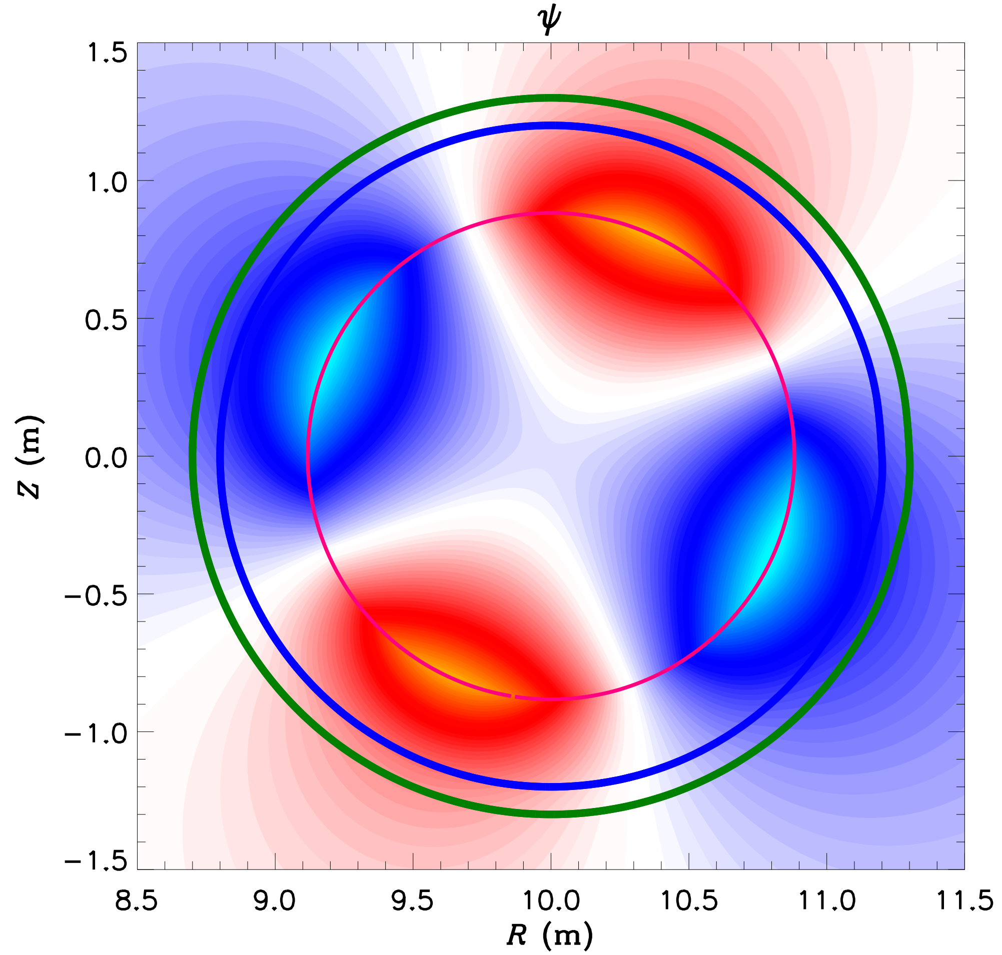

RWM Benchmark: M3D-C1 Agrees with Analytic Result

- **Growth rate calculated using linear, time-dependent calculation**
- **M3D-C1 agrees with analytic growth rate in both resistive-wall ($\tau_A << \tau_W$) and no-wall ($\tau_W << \tau_A$) limits**

Resistive-Wall Limit

B_θ Eigenfunction

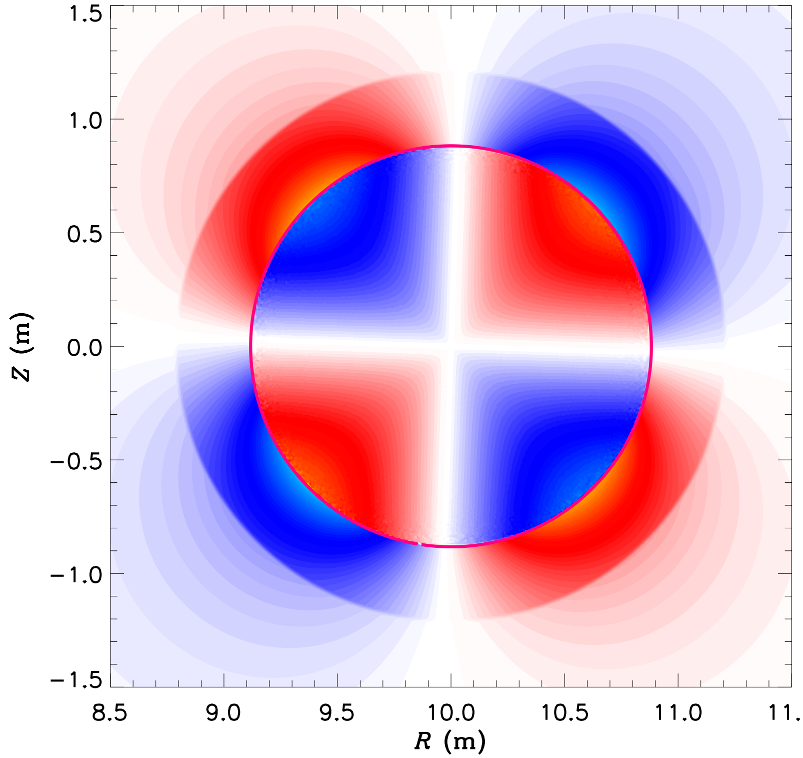

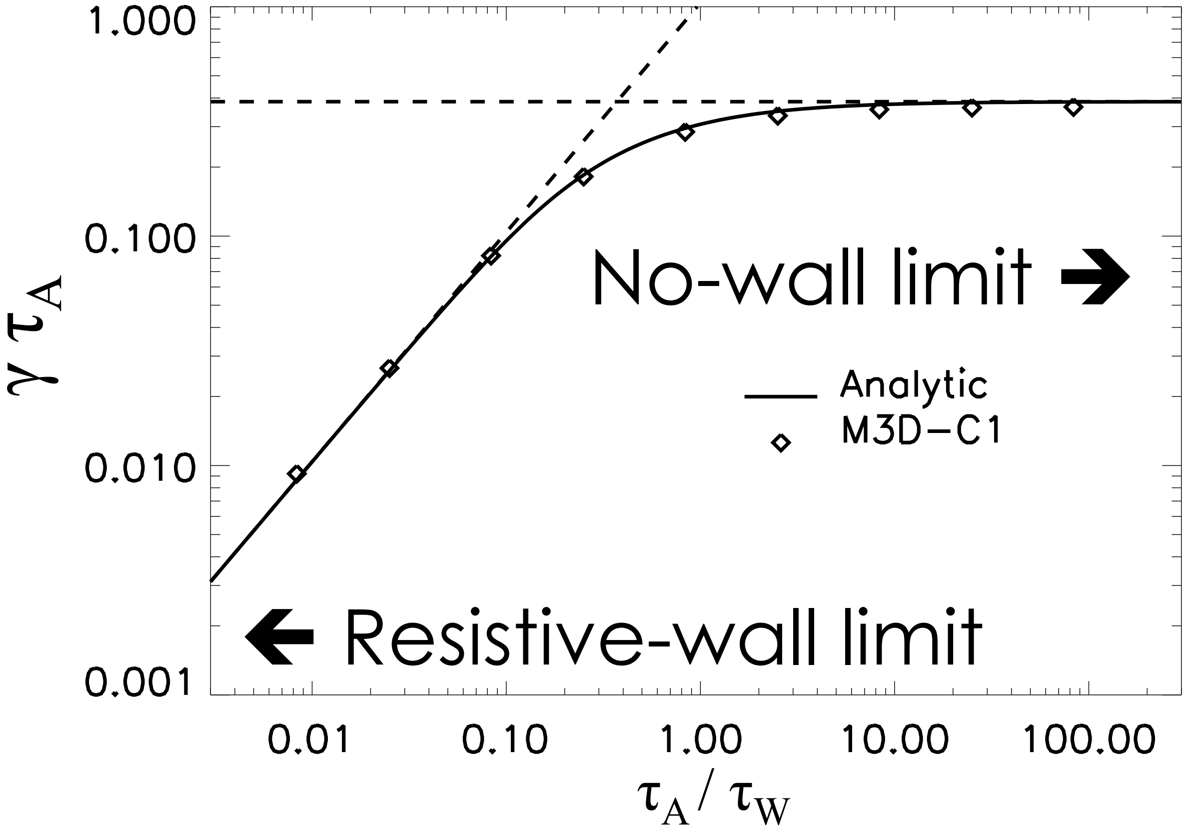

No-Wall Limit

B_θ Eigenfunction

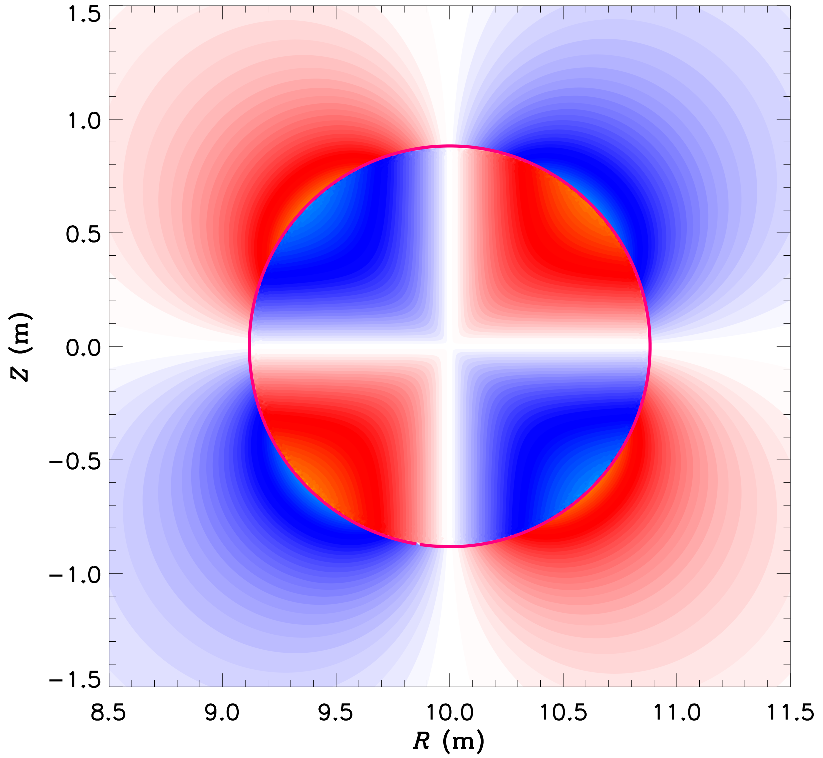

M3D-C1 Model Verified For Arbitrary Wall Thickness

- **Allowing arbitrary wall thickness leads to straightforward modification of Liu *et al.* (thin wall) dispersion relation**

$$\frac{\nu}{m-nq_0} - \frac{1}{1-(a/b)^{2\mu}F} = \frac{(\gamma\tau_A)^2}{2}\frac{q_0^2}{(m-nq_0)^2}$$

$$\mu = |m| \qquad \alpha = \sqrt{2\gamma\tau_W b/d}$$

$$\nu = \mathrm{sgn}(m) \qquad \beta = (1+d/b)\alpha$$

General solution

$$F = \frac{I_{\mu-1}(\beta)K_{\mu-1}(\alpha) - I_{\mu-1}(\alpha)K_{\mu-1}(\beta)}{I_{\mu-1}(\beta)K_{\mu+1}(\alpha) - I_{\mu+1}(\alpha)K_{\mu-1}(\beta)}$$

Thin wall ($d \ll b$)

$$F \rightarrow \frac{\gamma\tau_W}{\gamma\tau_W + \mu}$$

- **M3D-C1 model in good agreement with analytic results for arbitrary wall thickness**

- **In ITER, $(\gamma\tau_W)(d/b) \sim 0.2$ ***
  - Growth rates ~ 20—50% larger than thin wall solution

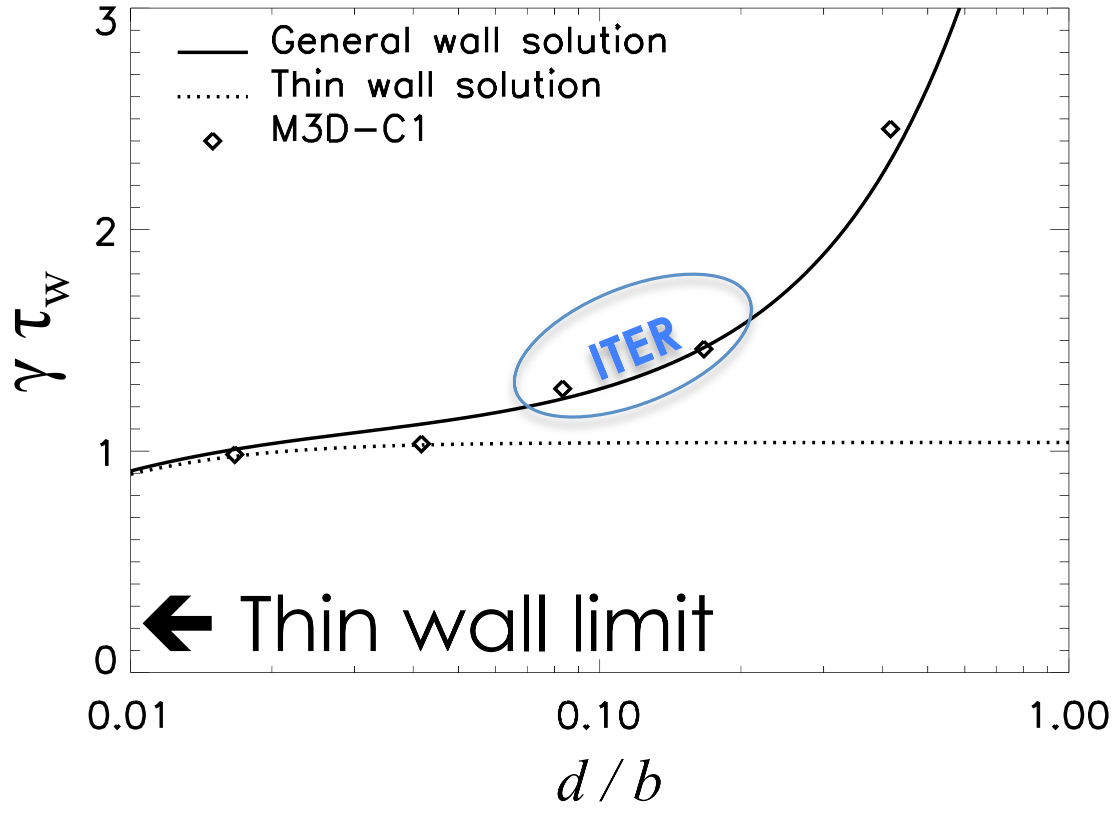

* F. Villone et al. *Nucl. Fusion* **50**, 125011 (2010)

Outline

- Resistive Wall Model in M3D-C1
- Verification Using Analytic Linear Resistive Wall Mode (RWM)
- **Free-Boundary Perturbed Equilibria**
- Vertical Displacement Event (VDE) Disruption

Resistive Wall Model Allows Free-Boundary Non-Axisymmetric Perturbed Equilibrium Solutions in M3D-C1

- **Resistive wall lets us calculate "free boundary" solution, because now conducting wall can be far from plasma**

- **New numerical methods in M3D-C1 have lead to improved solutions**
  - Fixed bug in boundary conditions
  - New version of meshing software allows higher resolution

Conducting wall

No $\mathbf{B}$ from plasma outside wall

Resistive Wall

$\mathbf{B}$ from plasma extends beyond wall

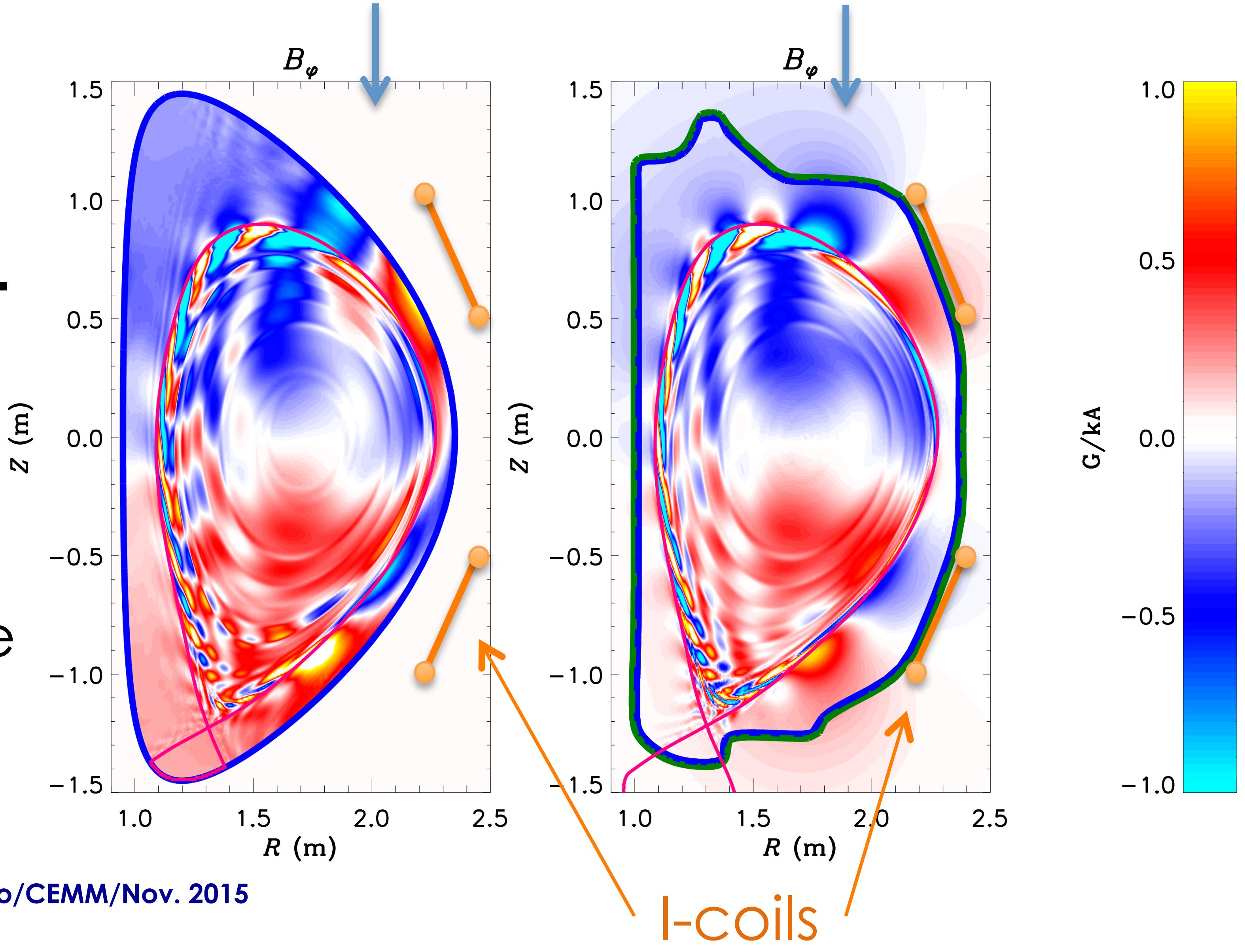

"Kink" Response is Similar in Free-Boundary Solution Relative to Conducting Wall Solution

- **"Kinking" is quantified by non-resonant components of B_{mn} ($m \neq nq$)**
  - Generic term indicating bending of magnetic surfaces without tearing

$$B_{mn} = \frac{(2\pi)^2}{A} \oiint \frac{\delta B \cdot \nabla \psi}{B_0 \cdot \nabla \theta} e^{im\theta - in\varphi}$$

$$B_0 = \nabla \psi \times \nabla \varphi + I \nabla \varphi$$

- **Kinking response is similar in both models**
  - Relative kinking depends on case, n

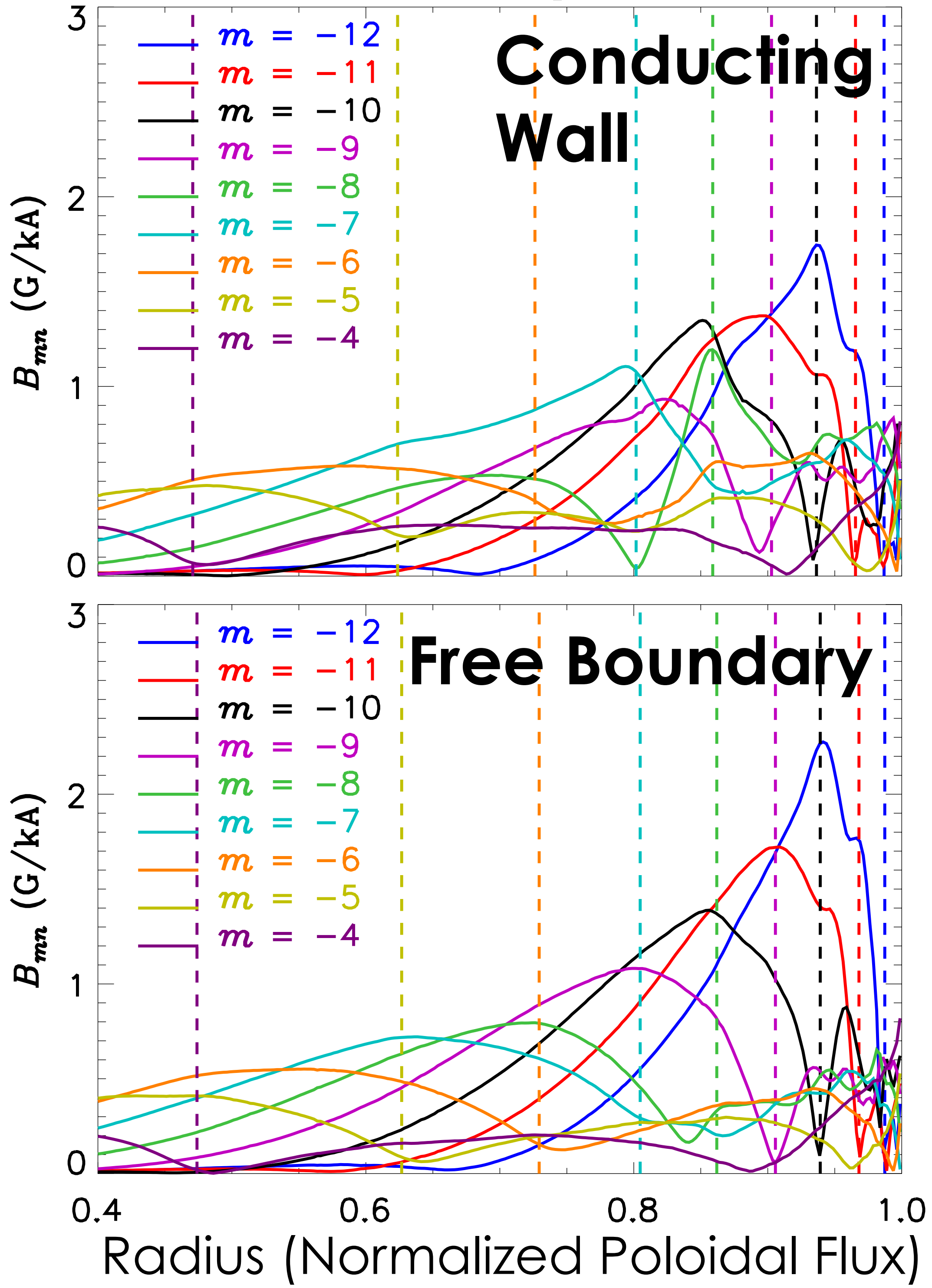

Tearing is Reduced in Free-Boundary Solution Relative to Conducting Wall Solution

- **New free-boundary solutions still find enhanced tearing response near $\omega_e = 0$, but ~3× less than in conducting wall case**
- **Why? Under investigation.**
  - Tearing mode is *more* stable with close conducting wall
  - Conducting wall constrains normal field closer to plasma → more drive for reconnection?
  - Weak tearing is consistent with free-boundary resistive MARS results

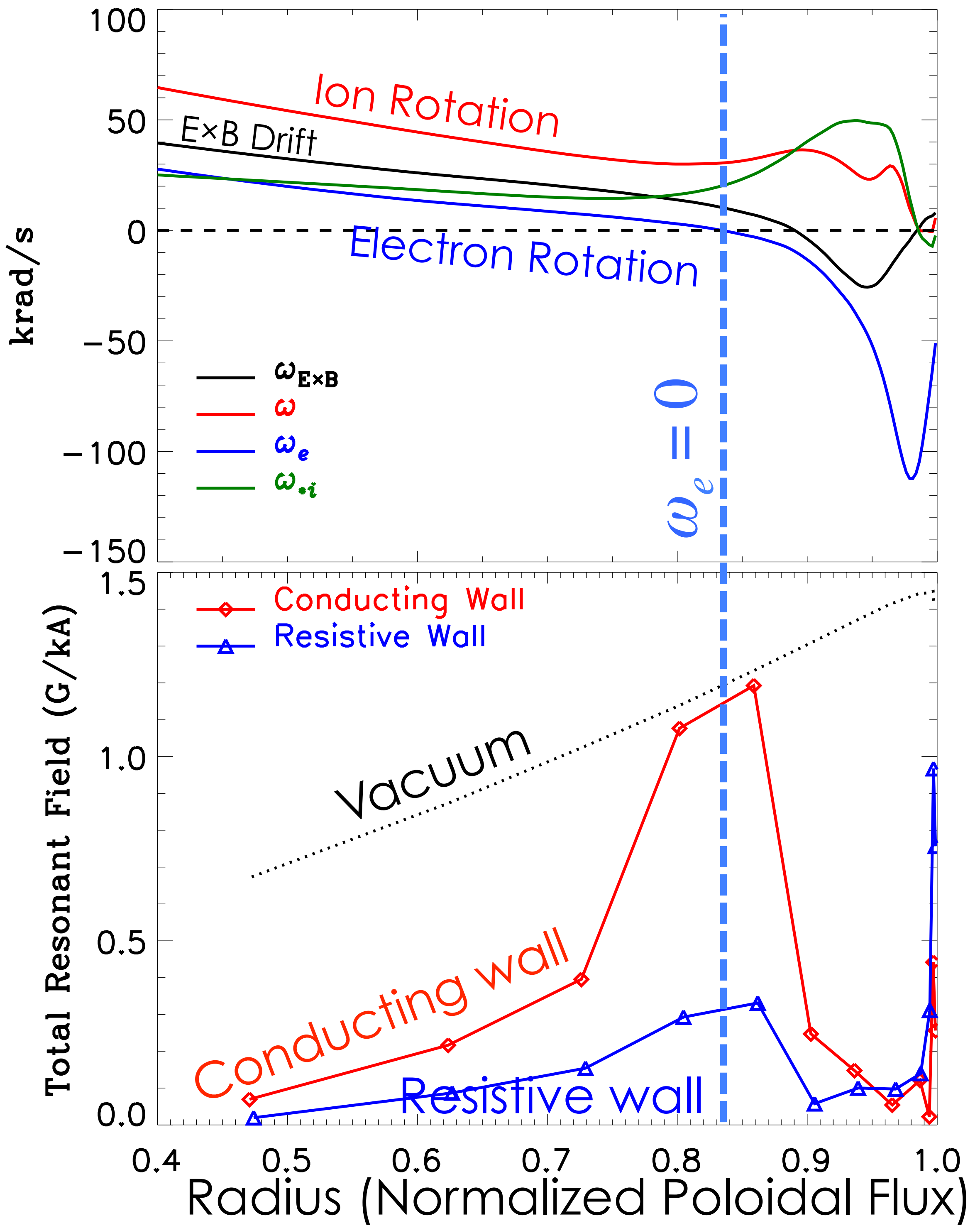

Outline

- Resistive Wall Model in M3D-C1
- Verification Using Analytic Linear Resistive Wall Mode (RWM)
- Free-Boundary Perturbed Equilibria
- **Vertical Displacement Event (VDE) Disruption**

Disruption Calculations Initialized using Vertically Unstable EFIT Reconstruction

- **Nonlinear calculation uses fairly realistic plasma parameters**
  - Spitzer resistivity: $S_0 \approx 6.8\times10^7$
  - Anisotropic thermal conductivity: $\chi_\parallel/\chi_\perp = 10^6$
  - Anomalous perp. transport: $100 < \chi_\perp < 800\ \mathrm{m}^2/\mathrm{s}$

- **RW region approximates first wall, not vacuum vessel here**

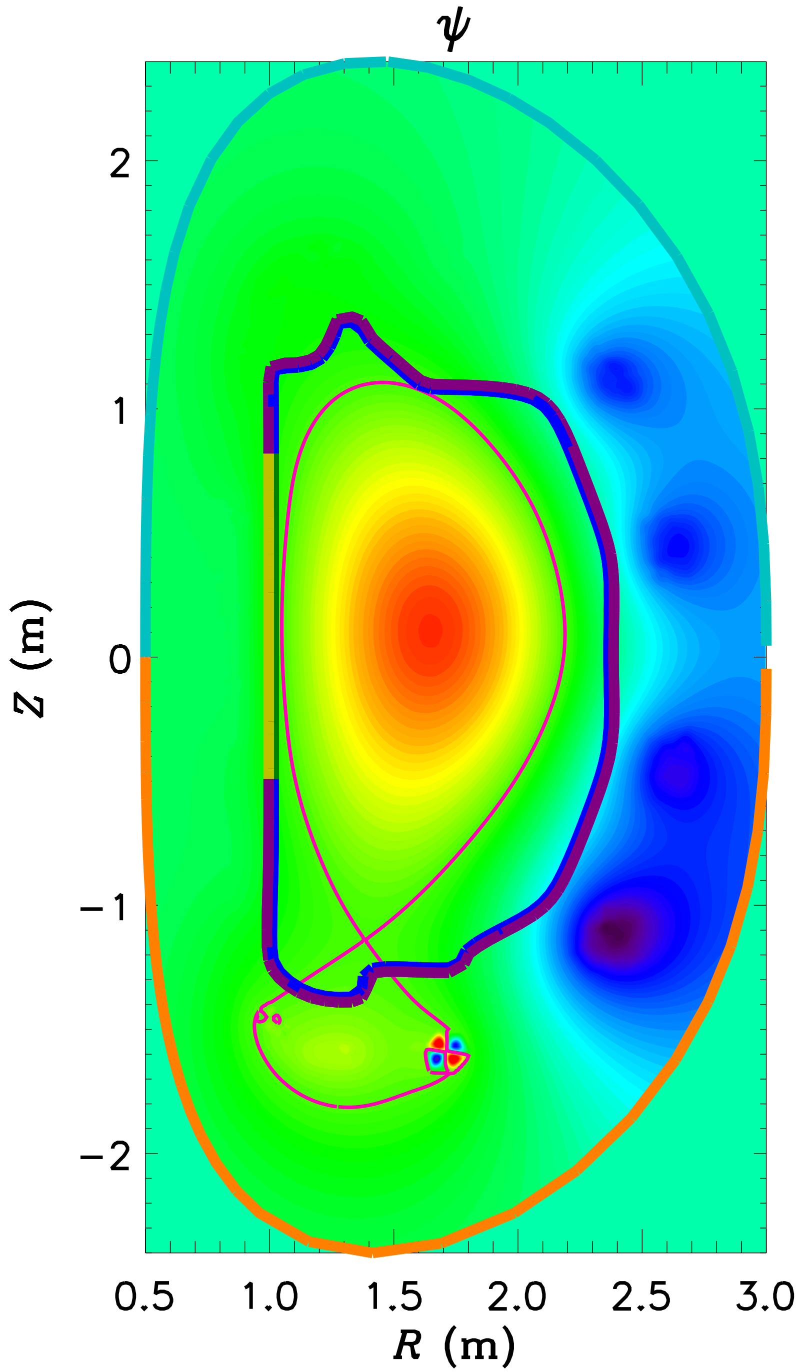

Simulations Include Simplified Thermal Quench (TQ) Phase

- **Thermal quench happens on ~100 μs timescale, due to large perpendicular thermal conductivity**
  - TQ phase not meant to be physically realistic! We are interested in current quench (CQ) phase

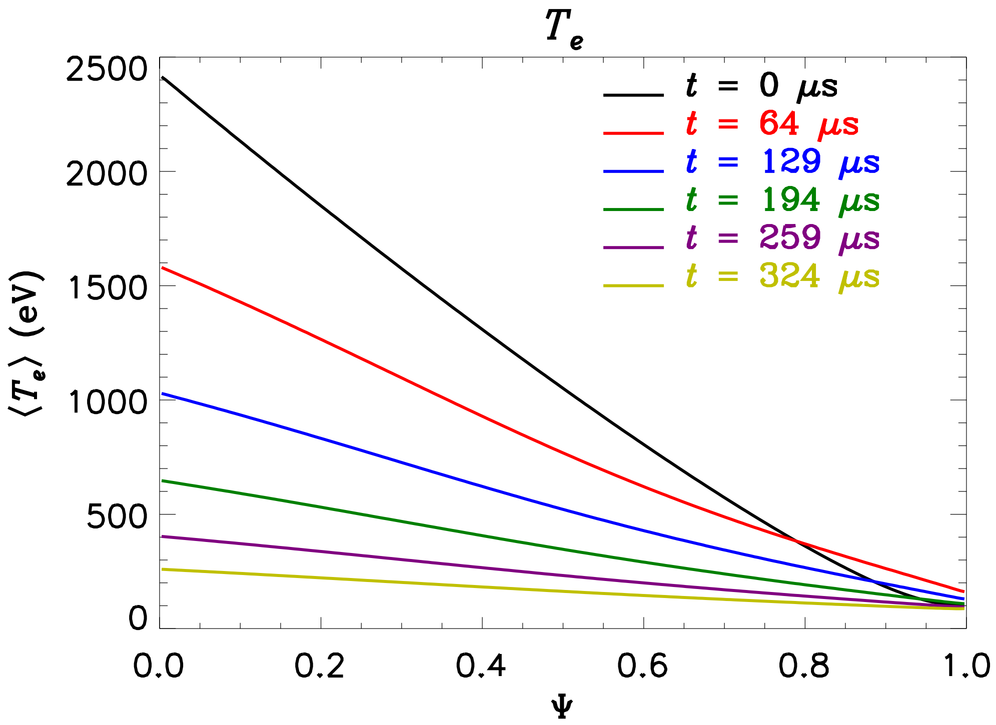

Axisymmetric Simulations Show Fast Thermal Quench, Slower Vertical Displacement Event (VDE)

- **Timescale of VDE Determined by Wall Resistivity (η_W)**

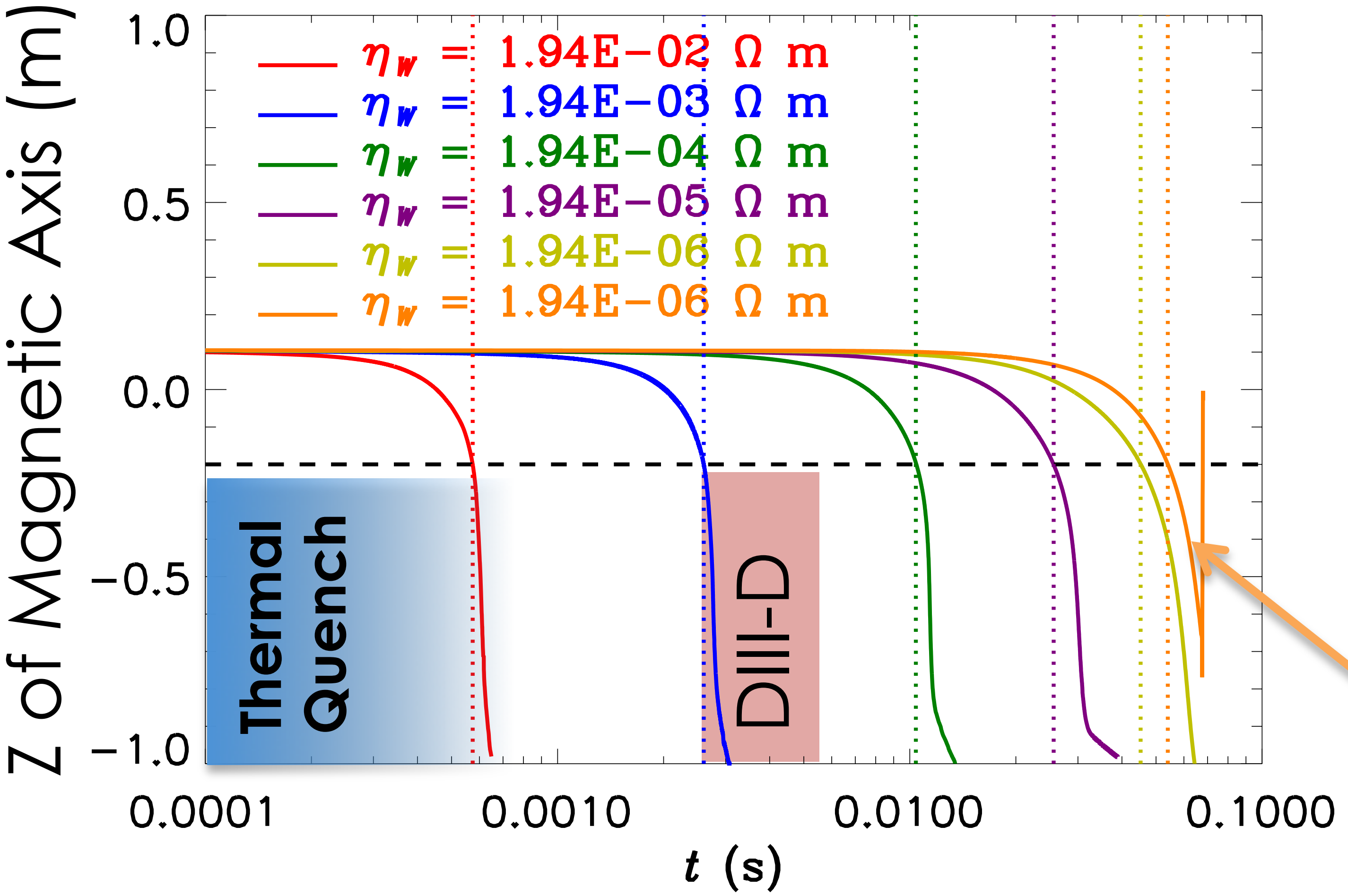

$\chi/10, T_{SOL}/2$

- **Physically realistic VDE timescale in DIII-D is a few ms**
  - Simulations bracket this regime
- **Timescale weakly dependent on parameters other than η_W**

Strong Currents form in Halo Region; Stabilizing Response Currents form in Wall and SOL

- **Both co-IP (Halo) and counter-IP ("Hiro") currents are seen in the open field-line region**

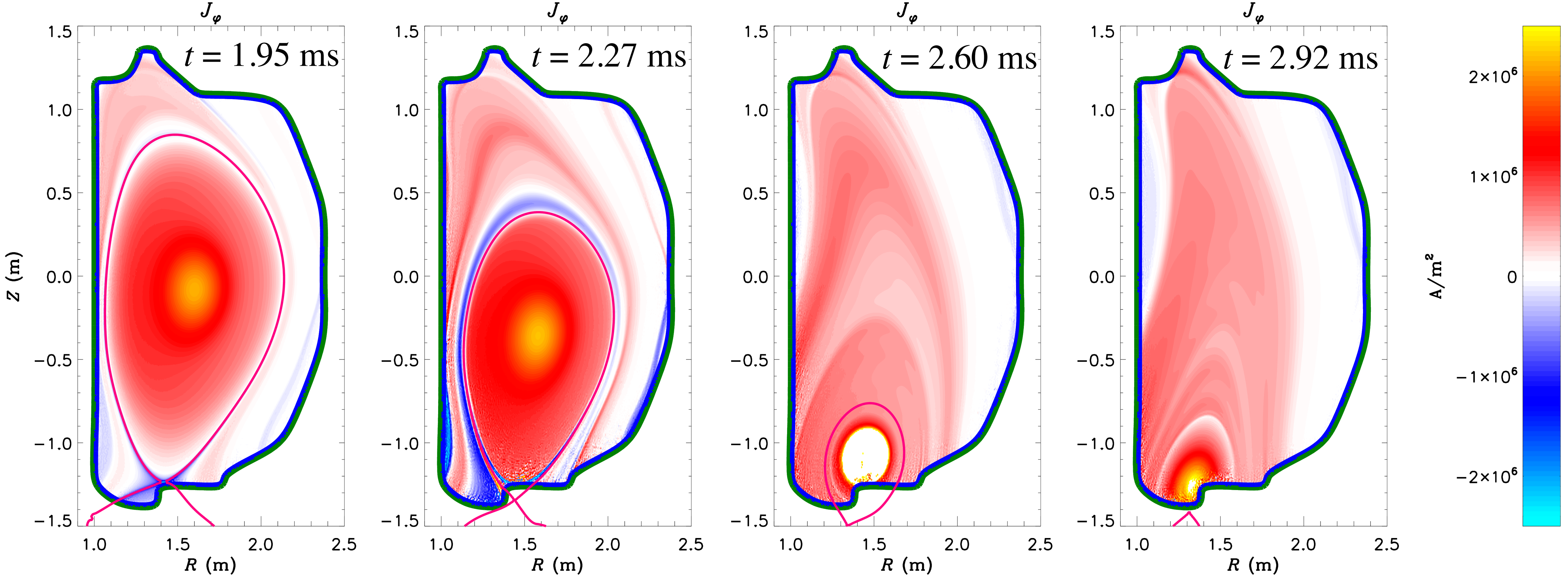

Relative Strength of Currents in Wall and Open Field-Line Region Change with η_W

- **At early stage of VDE, currents in the wall are stronger at lower η_W**
- **Counter-I_P currents are significantly stronger at higher η_W due to fast motion**

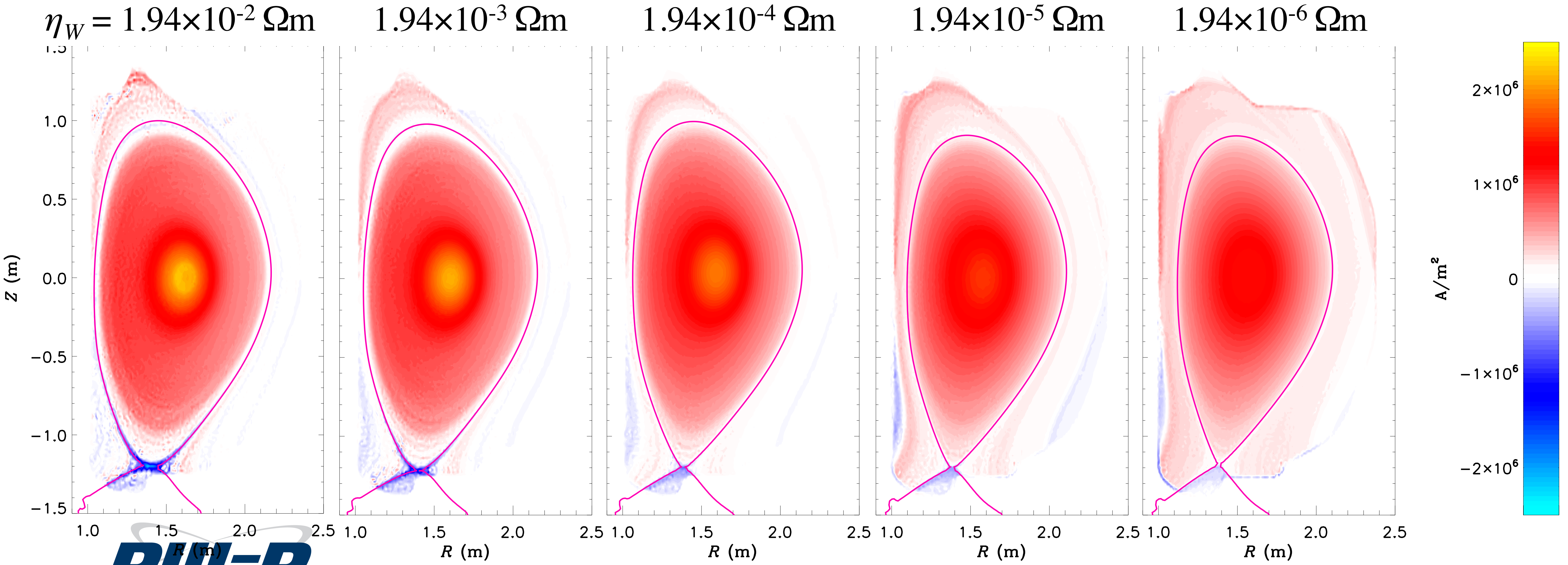
$\eta_W = 1.94\times10^{-2}\ \Omega\text{m}$ $1.94\times10^{-3}\ \Omega\text{m}$ $1.94\times10^{-4}\ \Omega\text{m}$ $1.94\times10^{-5}\ \Omega\text{m}$ $1.94\times10^{-6}\ \Omega\text{m}$

Current Spike Observed Before Current Quench; Associated with Vertical Motion of Plasma

- **Current spike occurs soon after plasma makes contact with the wall**
- **There is no spike associated with the thermal quench**
- **Spike is smaller when $\eta_W < \eta_{SOL}$**

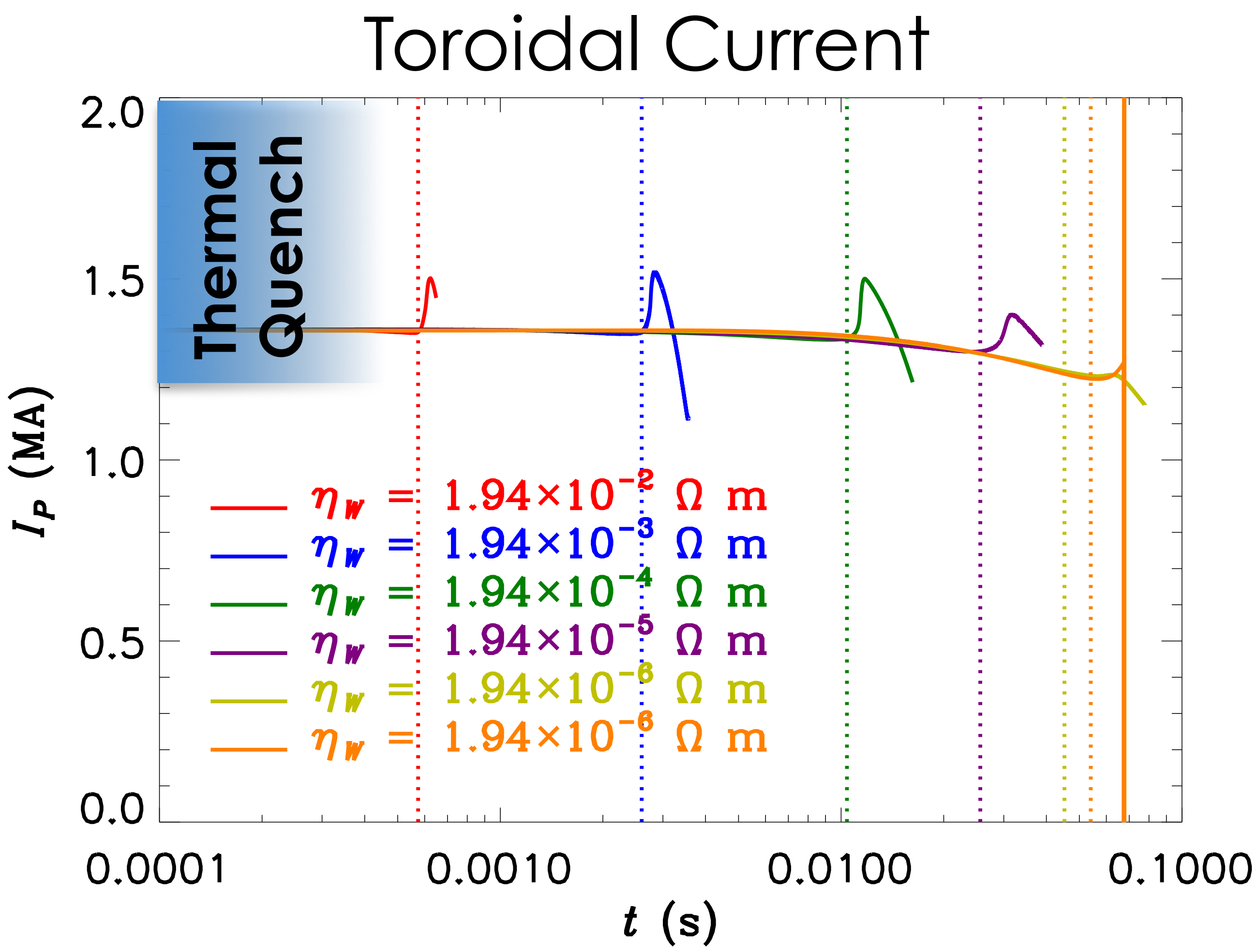

Current Spike Results from Loss of Induced Counter-I_P Currents When Plasma Contacts Wall

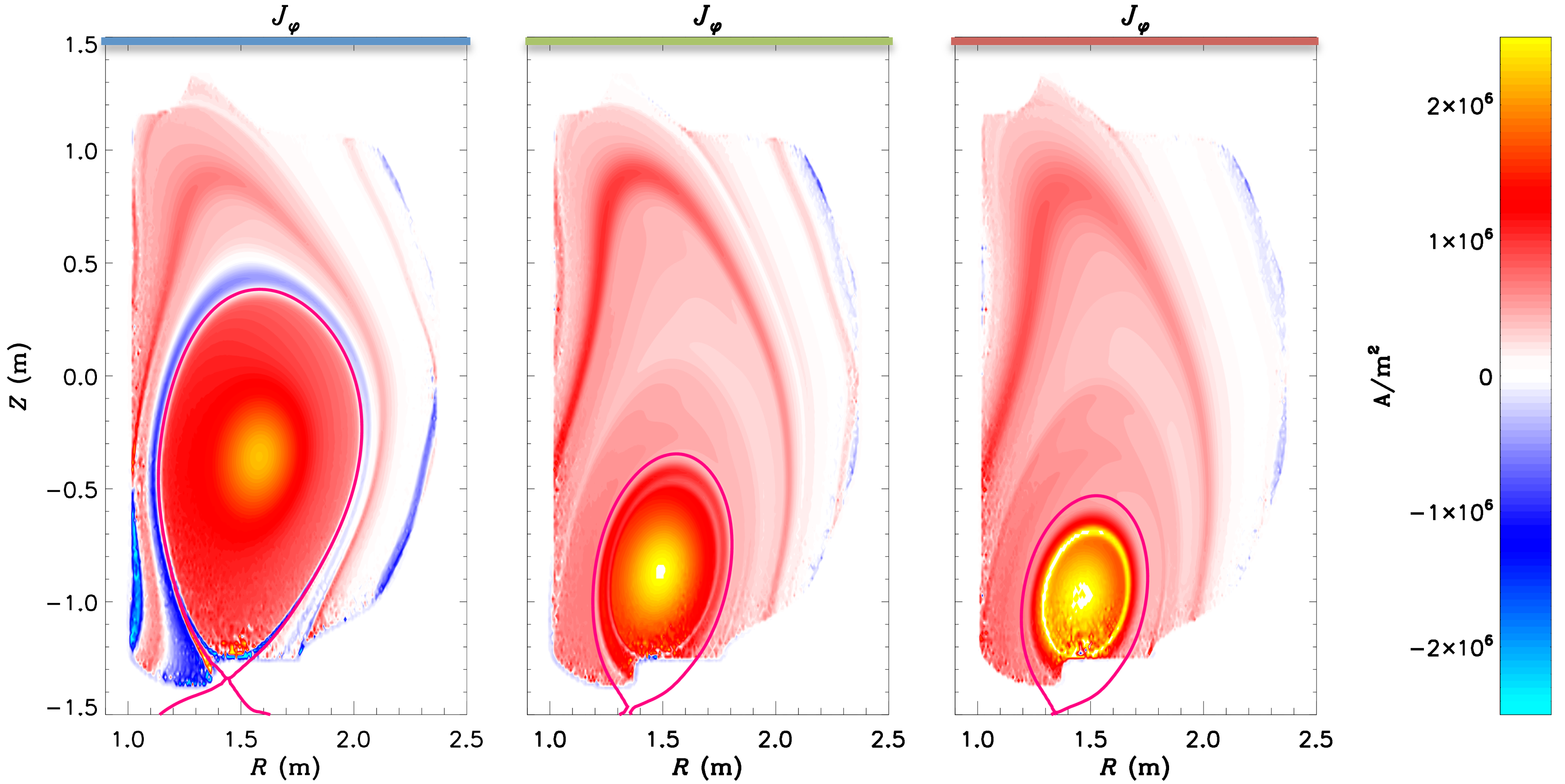

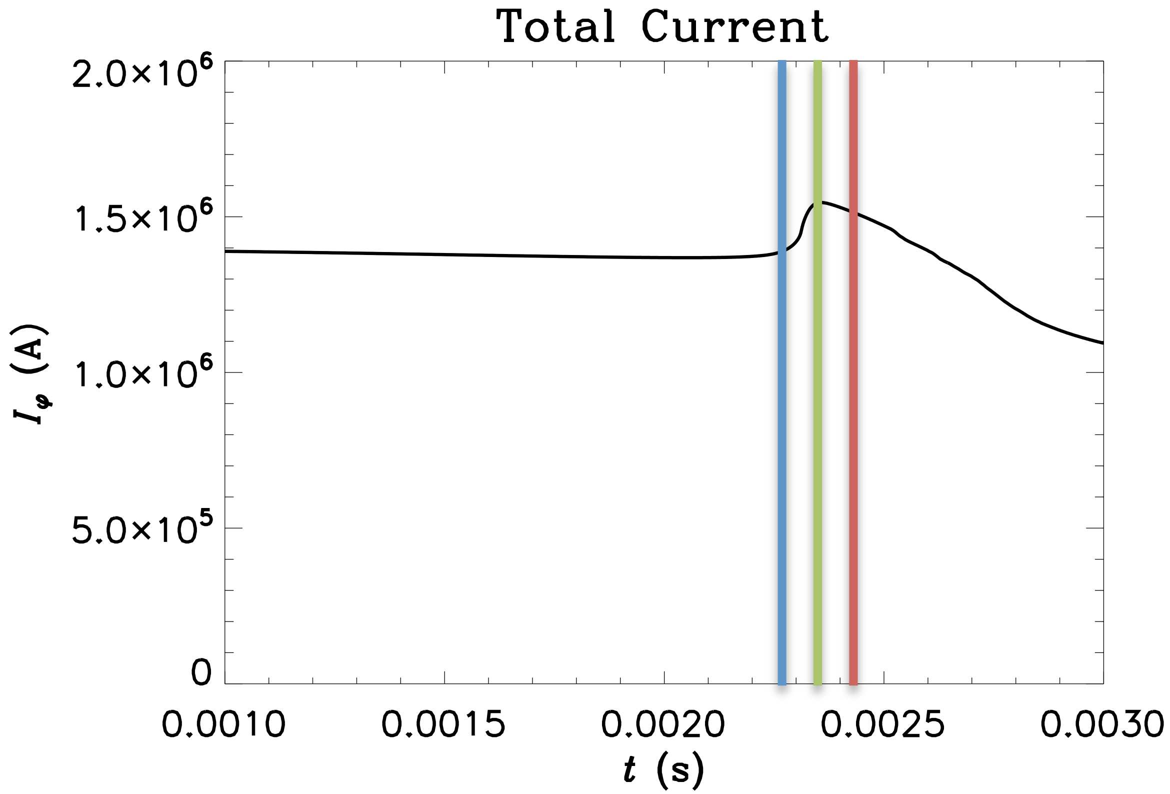

$$\eta_W = 1.94\times10^{-3}\ \Omega\ \mathrm{m}$$

- **Counter-IP** response currents are induced by motion of leading edge of plasma
- When plasma contacts wall, these currents are lost and plasma rapidly shrinks

No Significant Non-Axisymmetry Until After Current Spike in 3D Simulations, when $q_{edge} < 2$

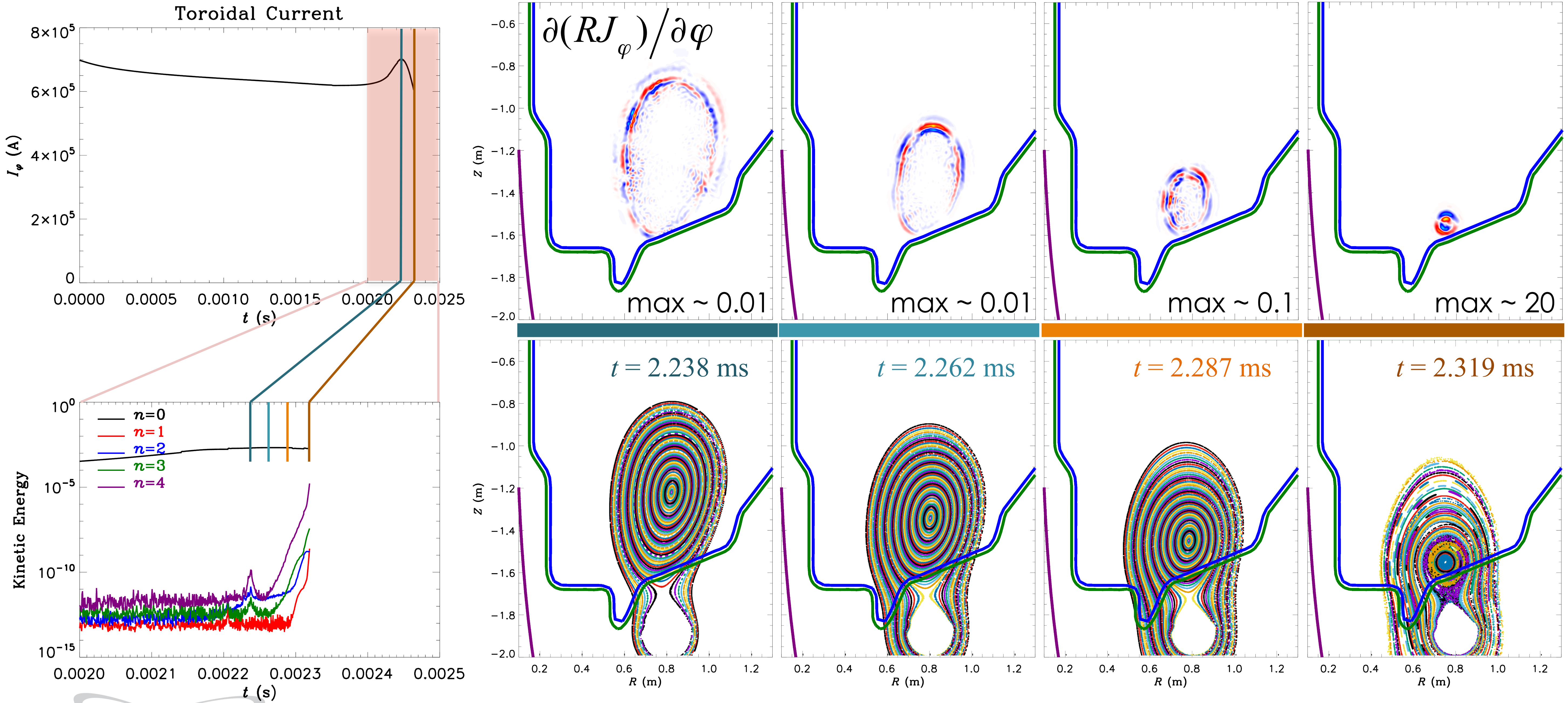

NM Ferraro/CEMM/Nov. 2015

M3D-C1 simulation from S. Jardin

Axisymmetric Forces Reach Maximum Just After Current Spike

- Forces peak at ~100 kN /m²
- Force distribution does not evolve significantly
- Currents in plasma are strong, but mostly force-free

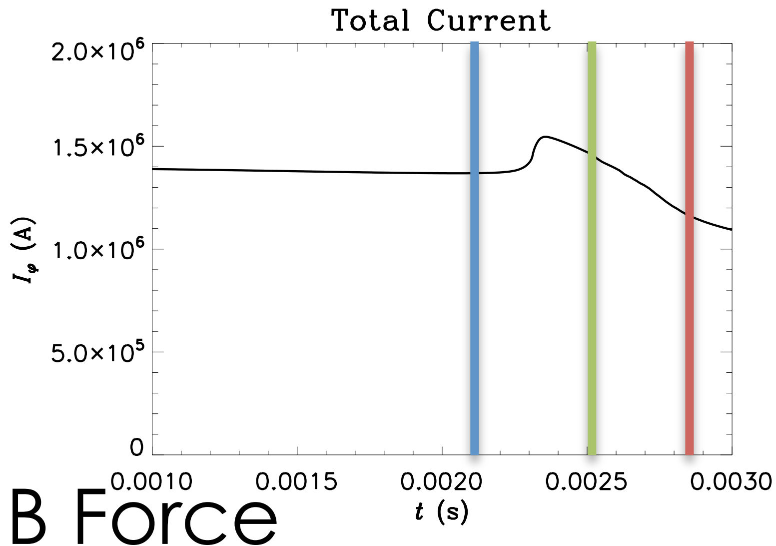

Radial J×B Force

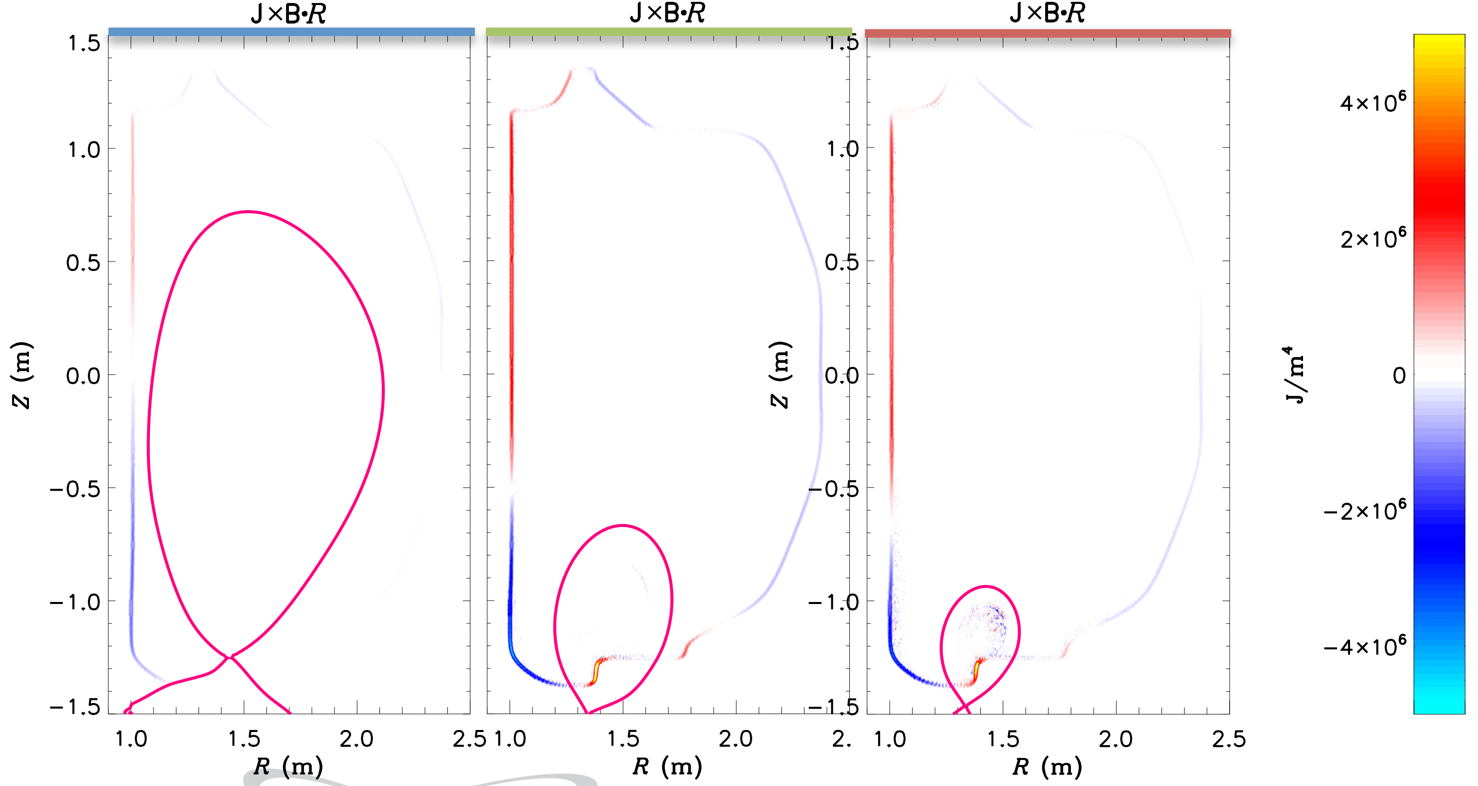

Vertical J×B Force

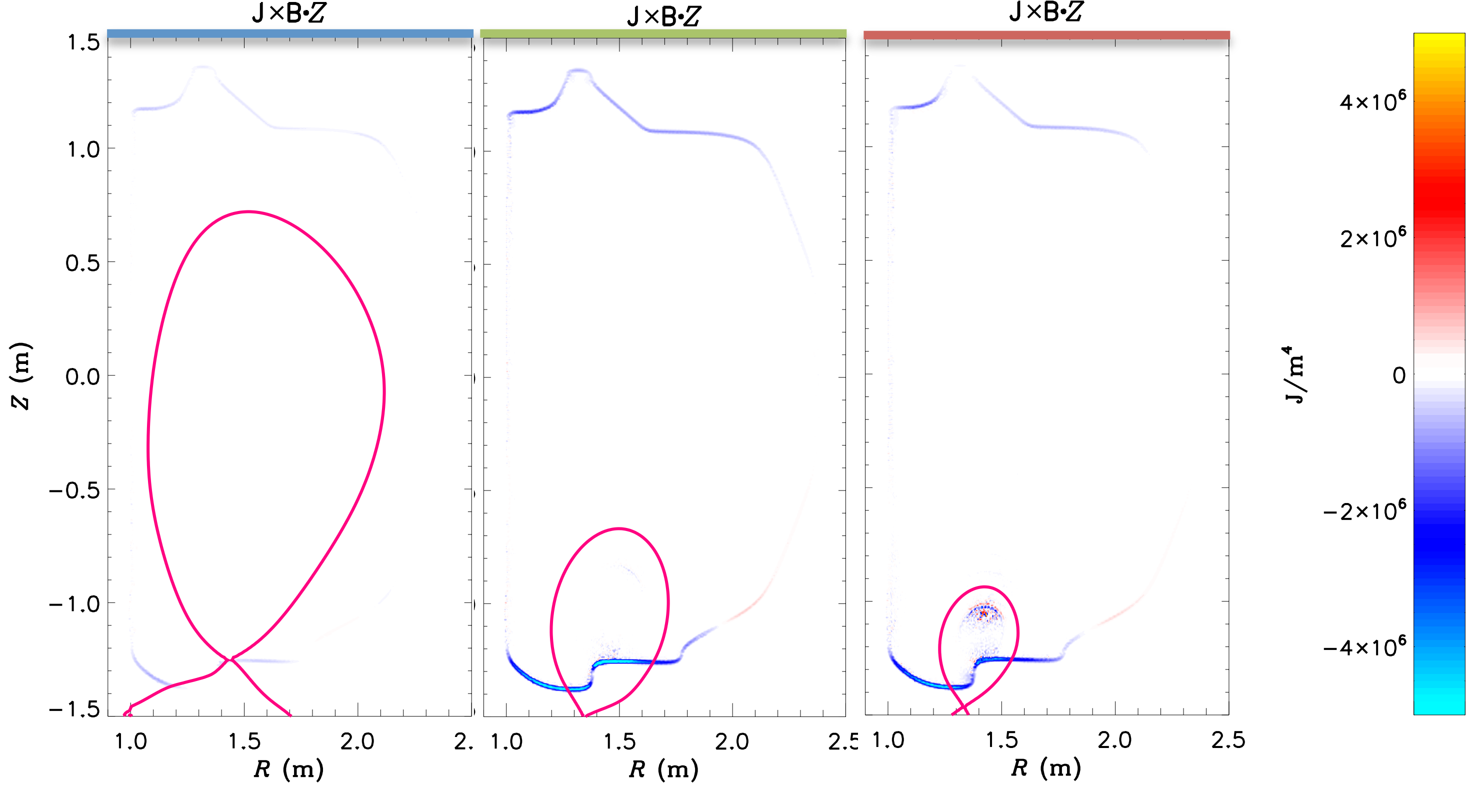

Maximum Halo Currents and Wall Force Depend Weakly on η_W

- Halo currents can exceed 100 kA/m^2
- Maximum Halo currents and force density in the wall is only weakly dependent on wall resistivity
- Impulse to vessel increases with τ_W because force is applied for longer time

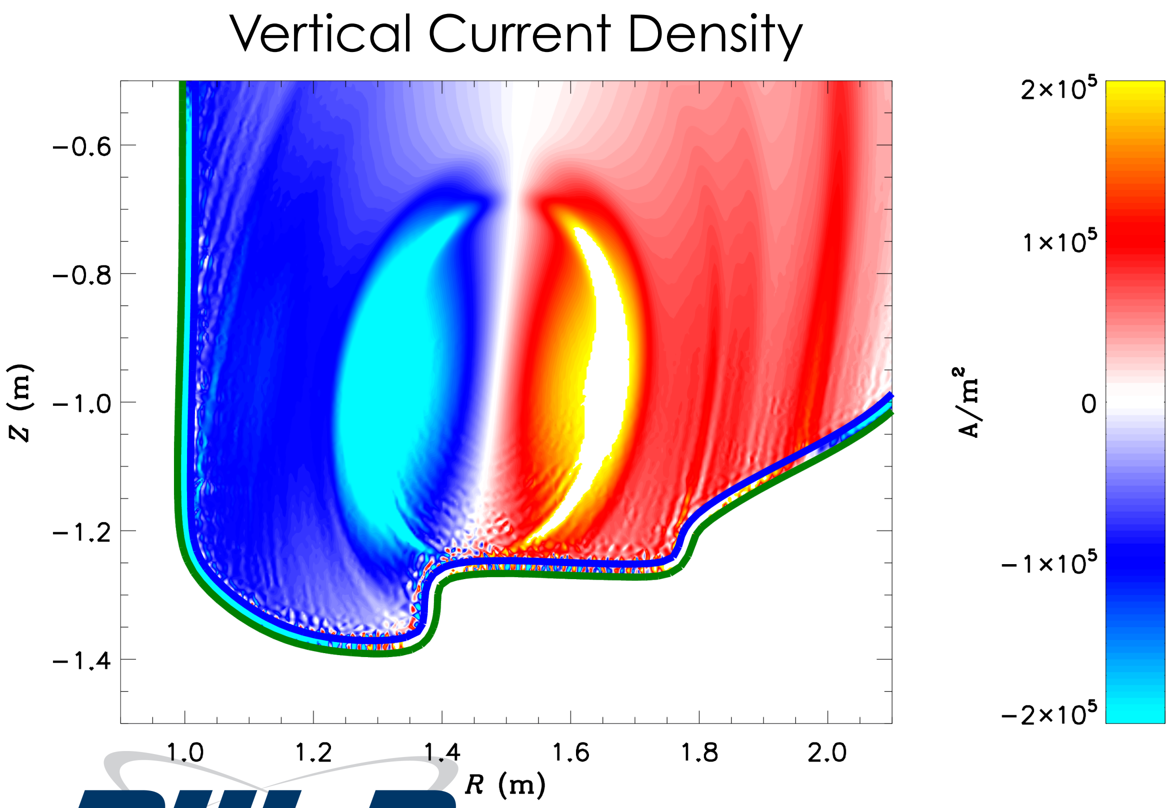

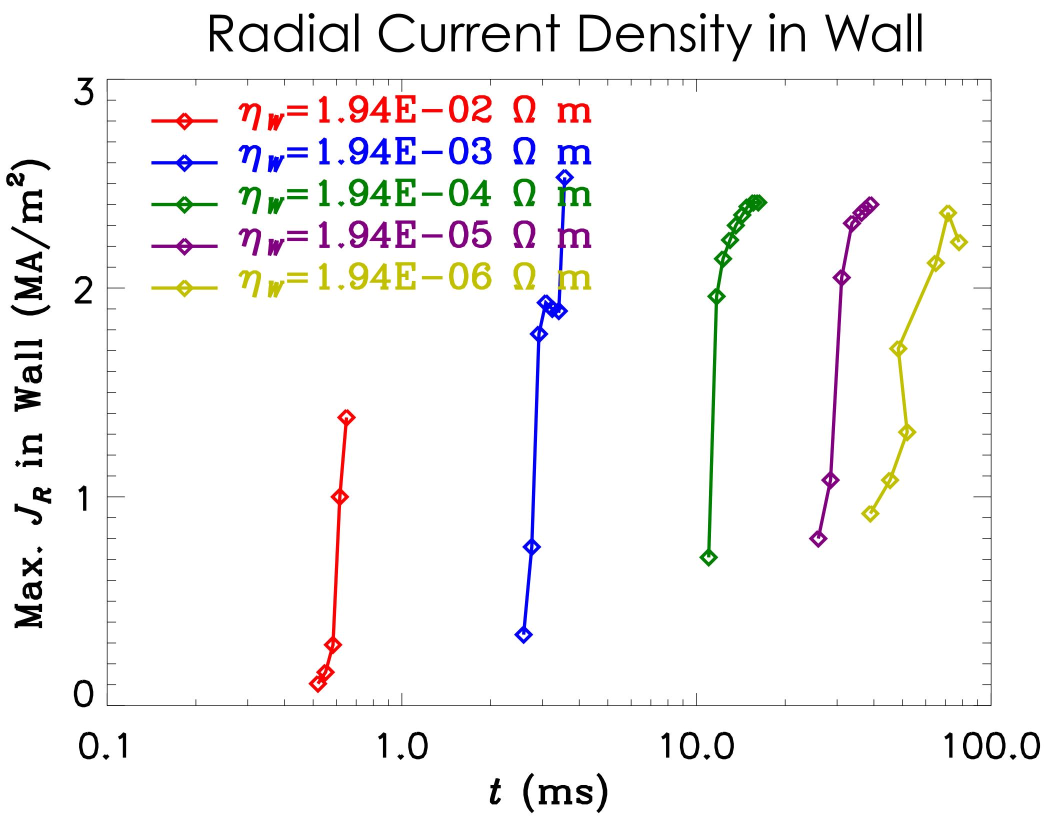

NM Ferraro/CEMM/Nov. 2015

Summary

- **New resistive wall model in M3D-C1 provides unique capability to calculate disruptive instabilities and disruption dynamics**
    - Halo currents are calculated without needing assumptions about halo width, SOL profiles, or magnetic topology
    - Model allows arbitrary wall thickness

- **Realistic VDE simulations allow quantification of currents & forces in wall**
    - Current spike in simulations are due to loss of response currents after plasma touches wall; not related to TQ
    - Maximum axisymmetric force depends weakly on τ_W, but impulse increases with τ_W
    - In 3D VDE simulations, plasma remains axisymmetric until $q_{edge} < 2$; quickly becomes dominated by 1/1 mode

- **Model provides new capability applicable to many areas of tokamak research**
    - Disruptions, RWMs, mode locking

Extra Slides

Resistive Wall Capability Allows Validation vs. Magnetics

- **Free-boundary calculations allow quantitative comparison with magnetic probes**
  - Probes are near boundary; conducting wall excludes plasma response

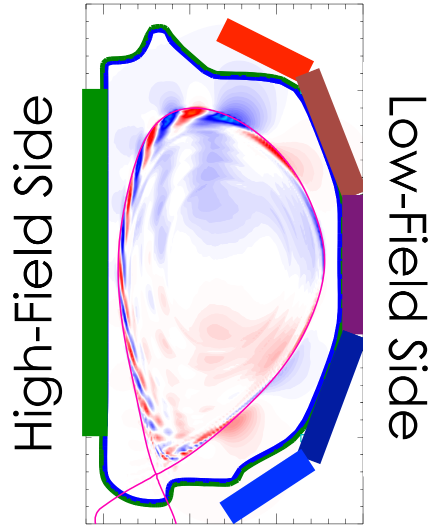

- **Validation performed as part of 2014 Joint Research Target**

- **Good agreement with magnetic probe data is found at low β_N, for n=1 and n=3**

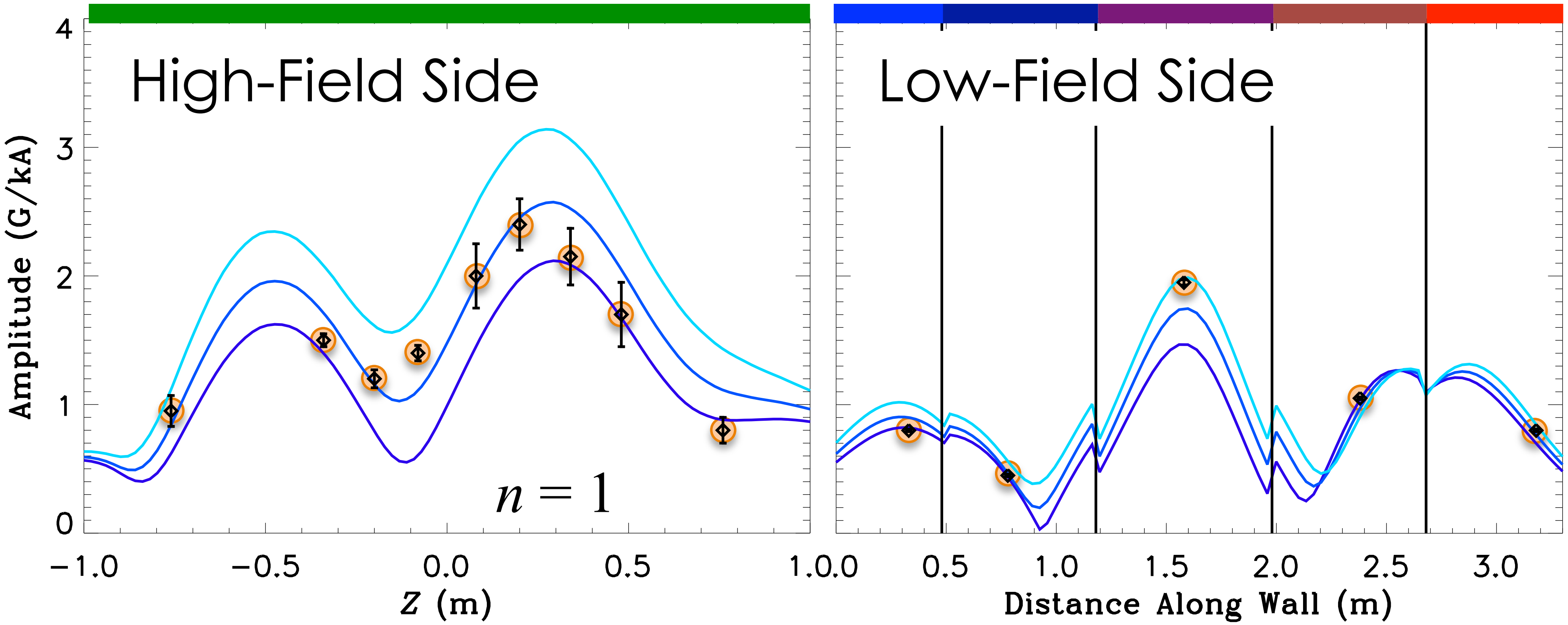

King, *et al. Phys. Plasmas* **22**, 072501

The IP Spike Results From Loss of Induced Counter-IP Currents When Plasma Contacts Wall

- **Axisymmetric force balance and $\nabla\cdot\mathbf{J}=0$ yield**

$$\mathbf{B}\cdot\nabla\left(\frac{J_\parallel}{B}\right)=0$$

- **Combining Ohm's Law and Faraday's Law and surface-averaging yields**

$$\mathbf{E}=-\mathbf{v}\times\mathbf{B}+\eta\mathbf{J}$$

$$\mathbf{E}=-\nabla\phi-\frac{\partial\mathbf{A}}{\partial t}$$

$$\Rightarrow$$

$$\frac{J_\parallel}{B}=-\frac{1}{\eta\langle B^2\rangle}\left\langle\mathbf{B}\cdot\frac{\partial\mathbf{A}}{\partial t}\right\rangle$$

$$\approx-\frac{RB_\varphi}{\eta\langle B^2\rangle}\left\langle\frac{1}{R^2}\frac{\partial\psi}{\partial t}\right\rangle$$

- **Counter-IP parallel current is driven by leading edge; Co-IP parallel current driven by trailing edge**

- **Eddy currents in wall also decrease after contact (more important at small η_W)**

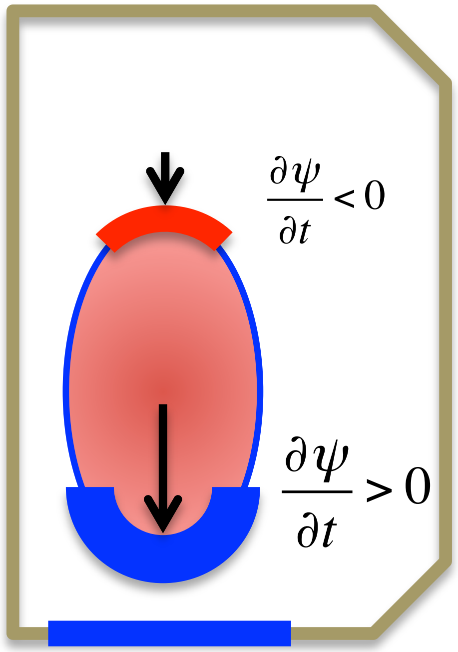

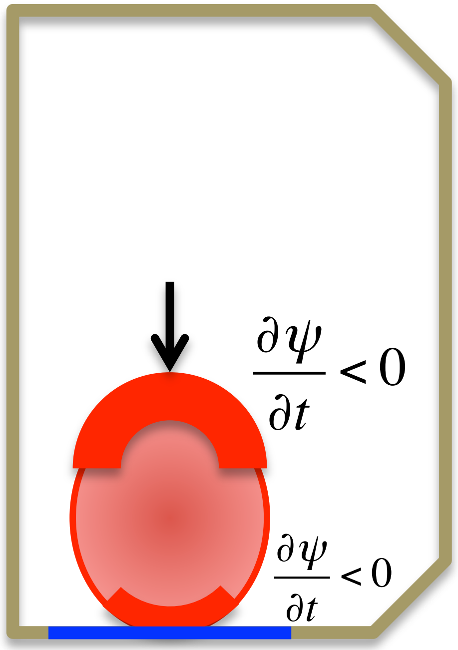

Before contact

- Parallel E at leading edge dominates
- $\frac{J_\parallel}{B}$ is counter-IP

After contact

- Parallel E at trailing edge dominates
- Parallel E at leading edge changes sign
- $\frac{J_\parallel}{B}$ is co-IP

q_{edge} Drops Below 2 Near Peak of Current Spike

- **q profile drops evolves as plasma shrinks**

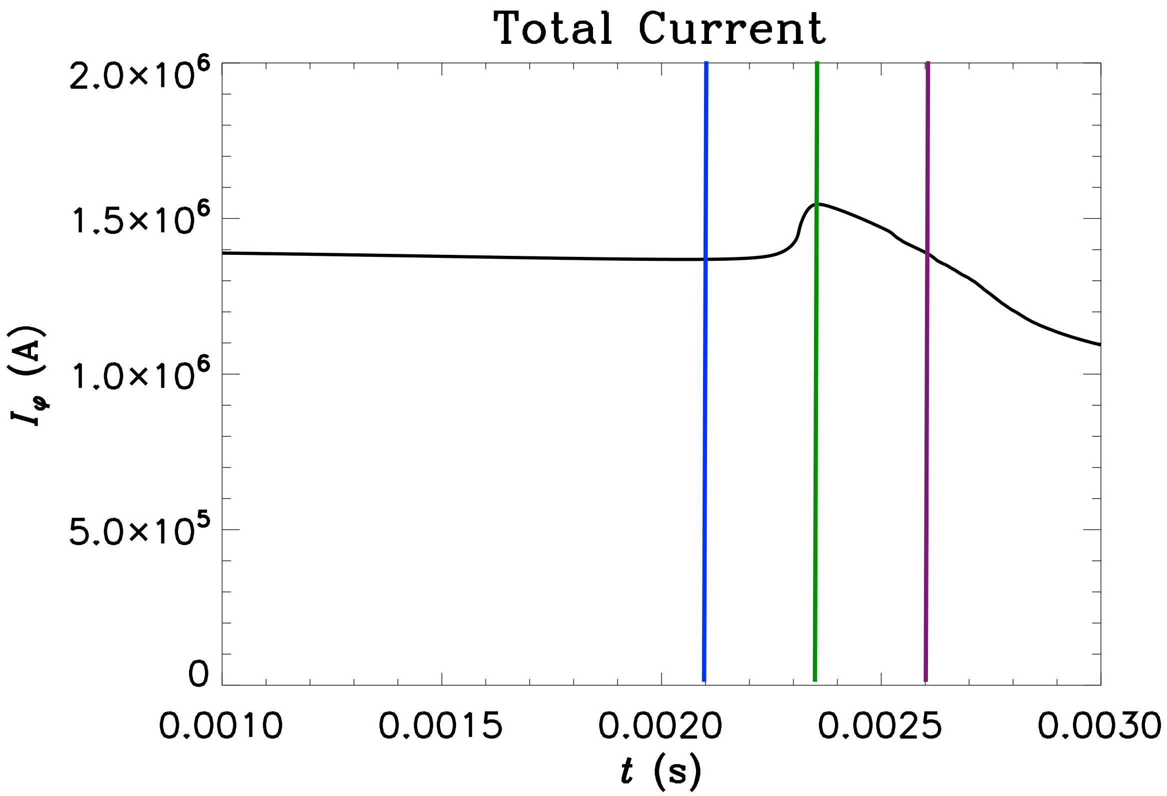

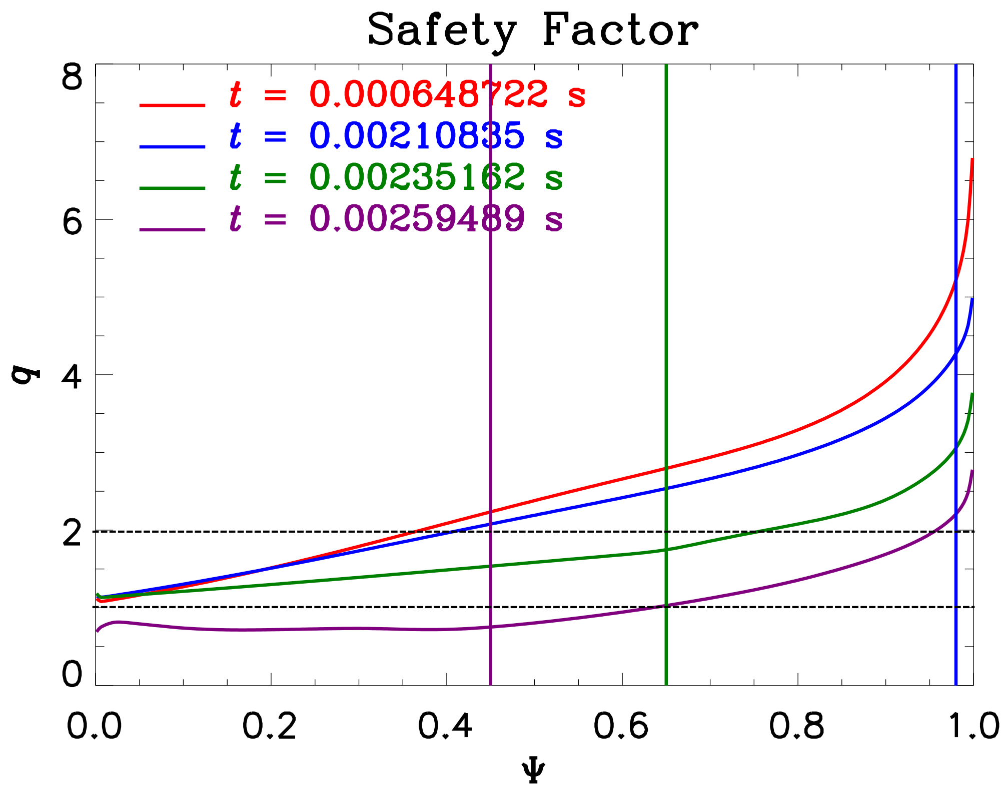

- **Vertical lines in q plot indicate plasma edge**

In C-MOD, Reconstructions Show Spike Before Plasma Contacts Wall

- **IP spike is seen at the initiation of the vertical displacement**

- **Halo currents peak at late stage of CQ**

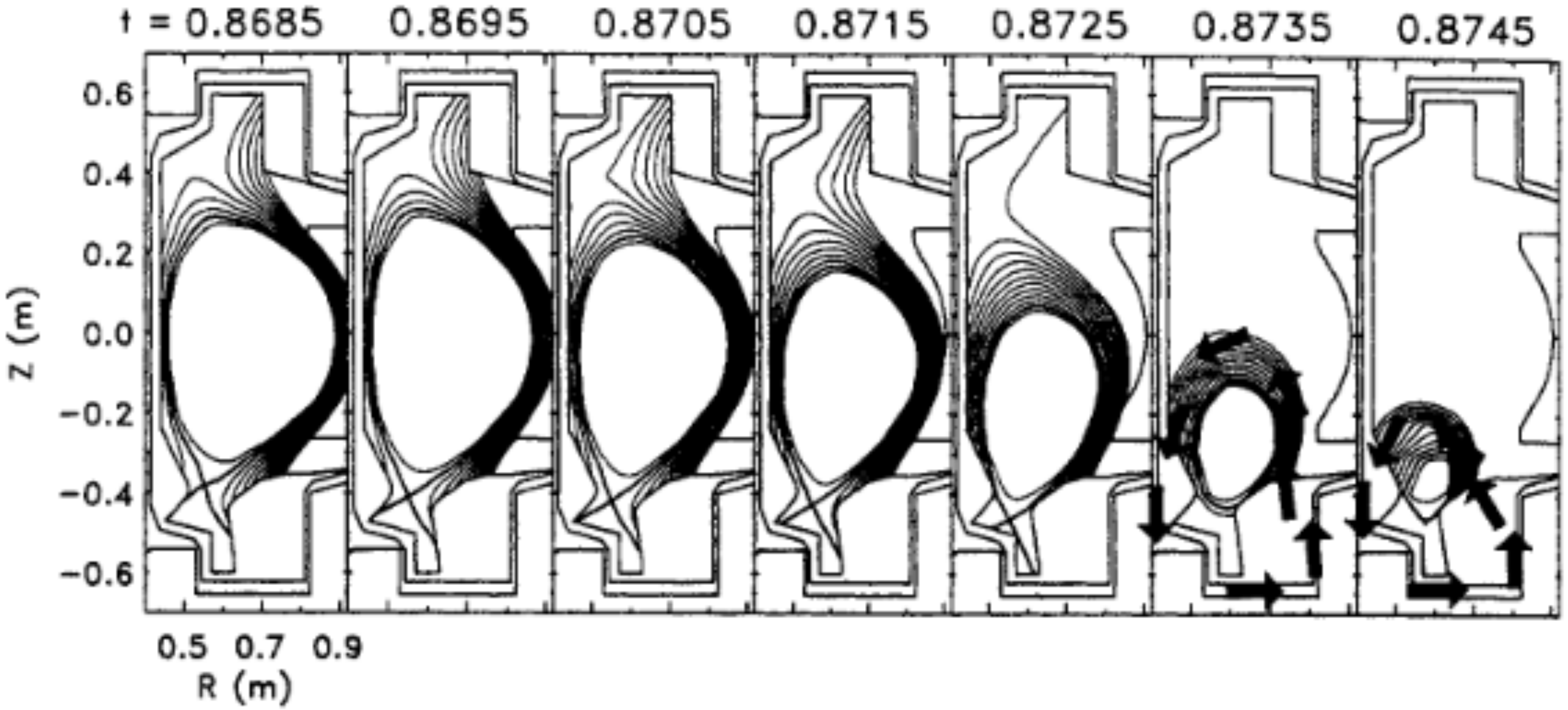

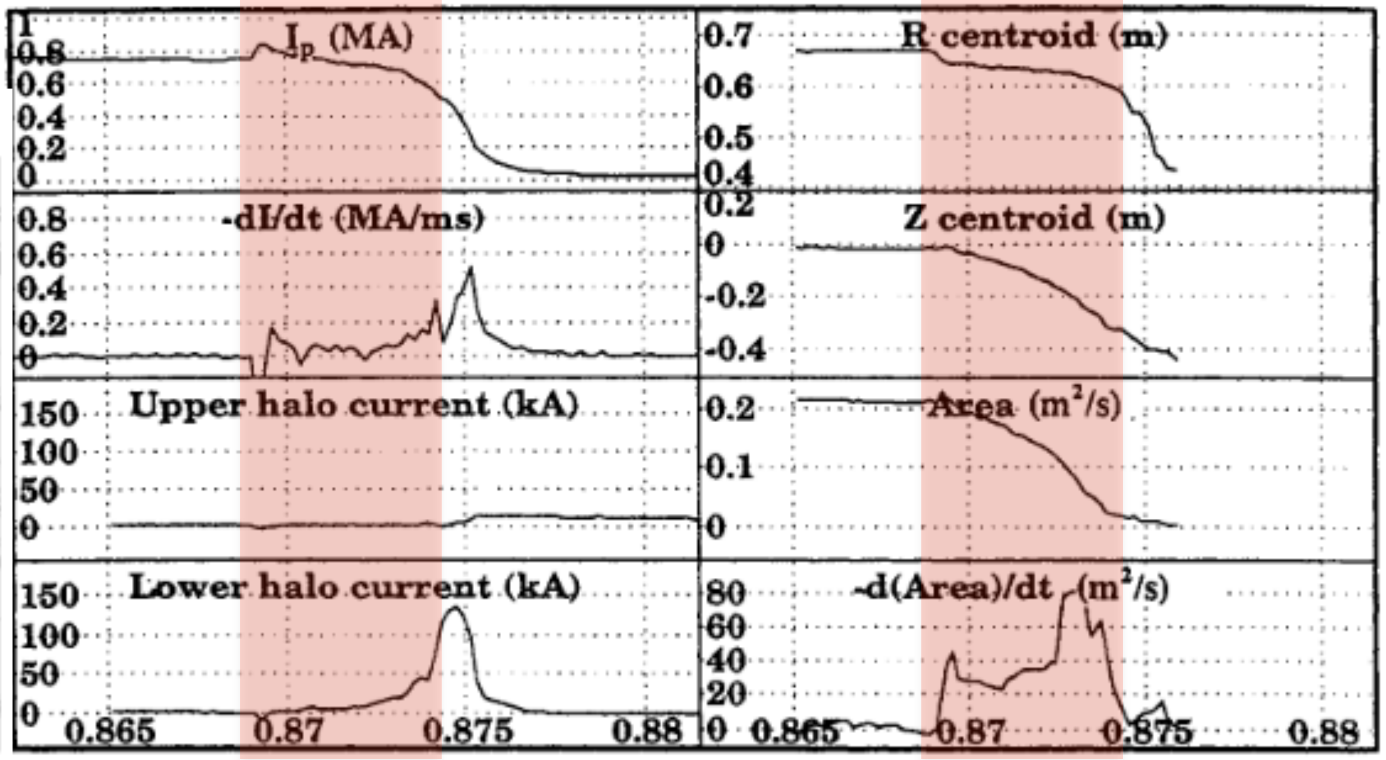

Wall Currents are Mostly Inductive

- **Currents are also present in the open field-line region**
  - Magnitude may be an artifact of high T_e in the open field-line region
  - Current flows from plasma to wall to ensure $\nabla \cdot \mathbf{J} = 0$
- **Wall currents are consistent with excluding poloidal flux**

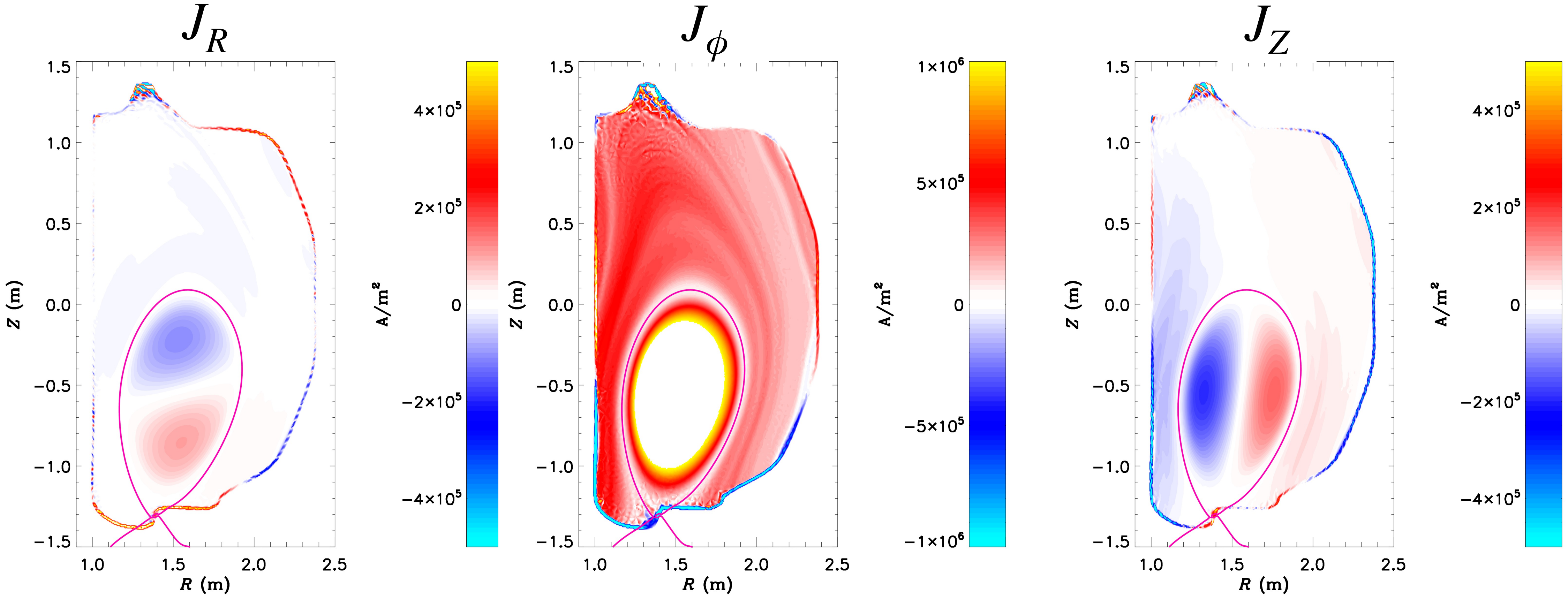

M3D-C1 Uses High-Order Elements on an Unstructured Mesh

- **The poloidal plane is discretized using triangular, C^1, degree-5 polynomial elements**

- **Linear calculations: a single toroidal Fourier mode is considered**

- **Nonlinear calculations: toroidal direction is discretized using cubic Hermite elements**
  - Preserves local coupling (block-tridiagonal)
  - Preserves C^1 property in all directions
  - Allows non-uniform toroidal resolution

- **(R, φ, Z) coordinates**